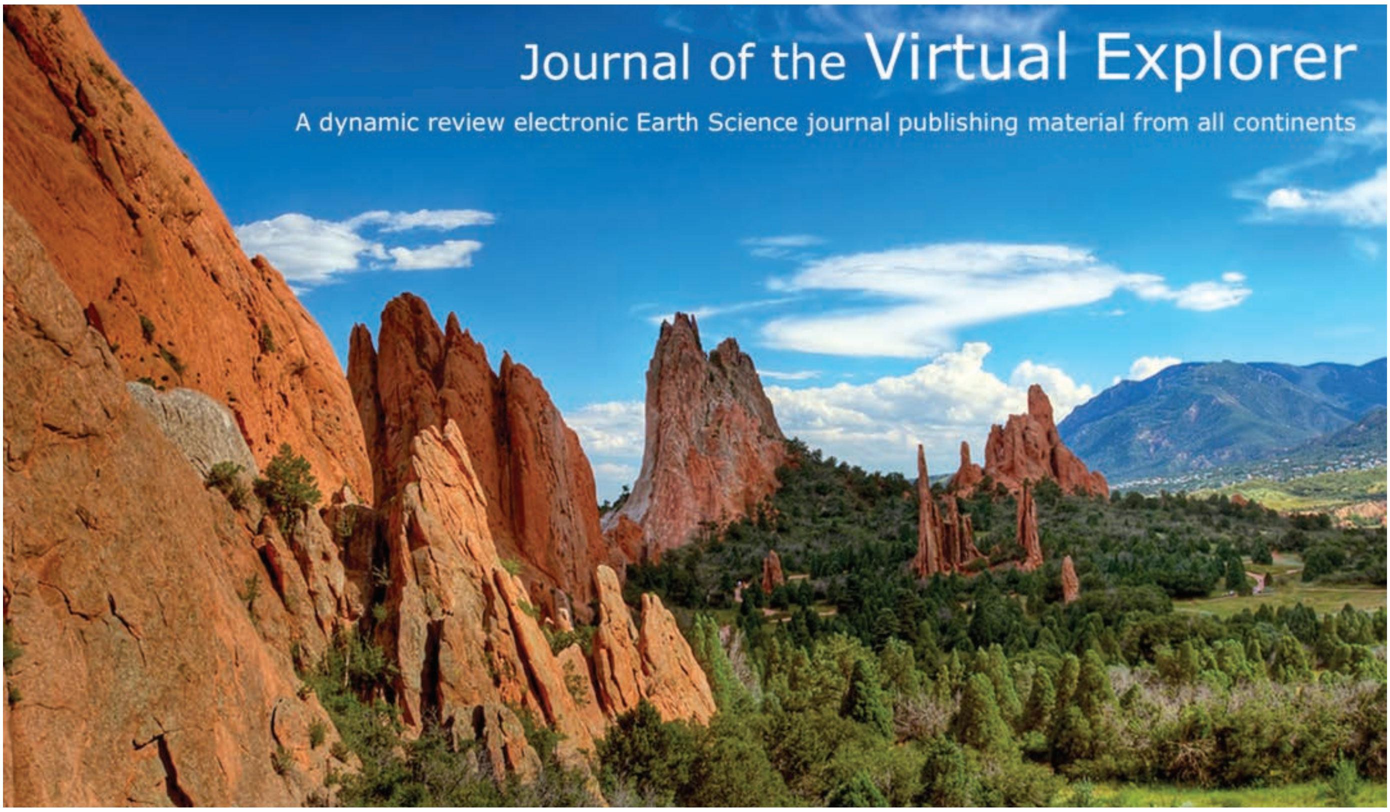

Virtual field guide for the Darjeeling-Sikkim Himalaya, India

Kellett D., Grujic D., Mottram C., Mukul M.

Journal of the VIRTUAL EXPLORER, Electonic Edition, ISSN 1441-8142, volume 47, Paper 5, DOI: 10.3809/jvirtex.2014.00344, In: (Eds) Chiara Montomoli, Rodolfo Carosi, Rick Law, Sandeep Singh, and Santa Man Rai, Geological field trips in the Himalaya, Karakoram and Tibet, 2014

Journal of the VIRTUAL EXPLORER

A dynamic review electronic Earth Science journal publishing material from all continents

Virtual field guide for the Darjeeling-Sikkim Himalaya, India

Kellett D.[1], *Grujic D.*[2], *Mottram C.*[3], *Mukul M.*[4]

[1] Geological Survey of Canada, 601 Booth Street, Ottawa, ON K1A 0E8, Canada.

[2] Department of Earth Sciences, Dalhousie University, Halifax, NS, Canada B3H 3J5.

[3] Department of Environment, Earth and Ecosystems, The Open University, Walton Hall, Milton Keynes, MK7 6AA.

[4] Department of Earth Sciences, Indian Institute of Technology-Bombay, Powai, Mumbai 400076.

GUIDE INFO

Keywords
South Tibet Detachment
Lesser Himalaya
Main Central Thrust
Strike-slip tectonics

Citation
Kellett , D., Grujic, D., Mottram, C. and Mukul, M. 2014. Virtual field guide for the Darjeeling-Sikkim Himalaya, India. In: (Eds.) Chiara Montomoli, Rodolfo Carosi, Rick Law, Sandeep Singh, and Santa Man Rai, Geological field trips in the Himalaya, Karakoram and Tibet, Journal of the Virtual Explorer, Electronic Edition, ISSN 1441-8142, volume 47, paper 5, DOI: 10.3809/jvirtex.2014.00344.

Correspondence to:
dawn.kellet@nrcan.gc.ca

IN THIS GUIDE

The Darjeeling-Sikkim Himalaya marks the beginning of the Eastern Himalaya. It is located between Bhutan to the east and Nepal to the west. In the west Sikkim shares Kanchenjunga, Earth's third highest mountain, with Nepal, while the ridge line forming Sikkim's eastern border flanks the Yadong-Gulu rift graben. The South Tibet detachment (STD) system with a small portion of the Tibetan plateau defines the northern boundary of the Darjeeling-Sikkim Himalaya while the Main Frontal fault system defines its southern boundary. The Main Boundary thrust (MBT), the Ramgarh thrust (RT) and the Main Central thrust (MCT) are other thrusts that are well-exposed in the area along a south to north, transport-parallel traverse. The Lesser Himalayan Duplex (LHD) with horses involving rocks from the RT and MBT thrust sheets stacked in a complex geometry dominates the Lesser Himalaya in the region. The puzzling MCT Zone, with two strands of the MCT, is a classical region of inverted metamorphic isograds, and new ideas about its tectonics will be introduced. Along-strike variations in the geometry and kinematics of the Darjeeling-Sikkim Himalaya is evident from the presence of a salient-recess pair separated by a transverse, sinistral strike-slip fault that cuts across the frontal thrust systems and extends into the Yadong-Gulu rift system. The seismicity in the region is dominated by transverse strike-slip tectonics as evident from moderate strike-slip earthquakes in the region since 1980 and 2011 in contrast with the Himalaya further west that is dominated by thrust seismicity. Out-of sequence neotectonic deformation is also seen in the frontal Darjeeling-Sikkim Himalaya. This virtual guide tours key outcrops at which field expressions of first-order Himalayan structures such as the MBT, MCT, STD system and the Gish fault can be observed. Sites of neo-tectonic activity and horses within the LHD are also visited.

1 INTRODUCTION TO SIKKIM-DARJILING

Sikkim is a small state of India situated between Nepal and Bhutan to the west and east, and Tibetan China and West Bengal to the north and south, respectively. A walk from Darjiling north through Sikkim to Thanggu and onto the Tibetan plateau follows ancient trade routes, as well as the earliest British expeditions to summit Everest, which required that the mountaineers travelled north from Darjiling up the Tista river valley to its headwaters before turning west to approach Everest via the Tibetan plateau. Figure 1.1 illustrates the geology and structures of the region based upon our recent mapping.

Although heavily vegetated, Sikkim is transected by several roads, providing abundant access to road cuts in both NS and EW transects, particularly in the southern half of the region, from the foreland basin in West Bengal north over the Main Frontal thrust and into the Tista river valley and its many tributaries (Fig. 1.1). In this guide, we present some of the key outcrop and field views

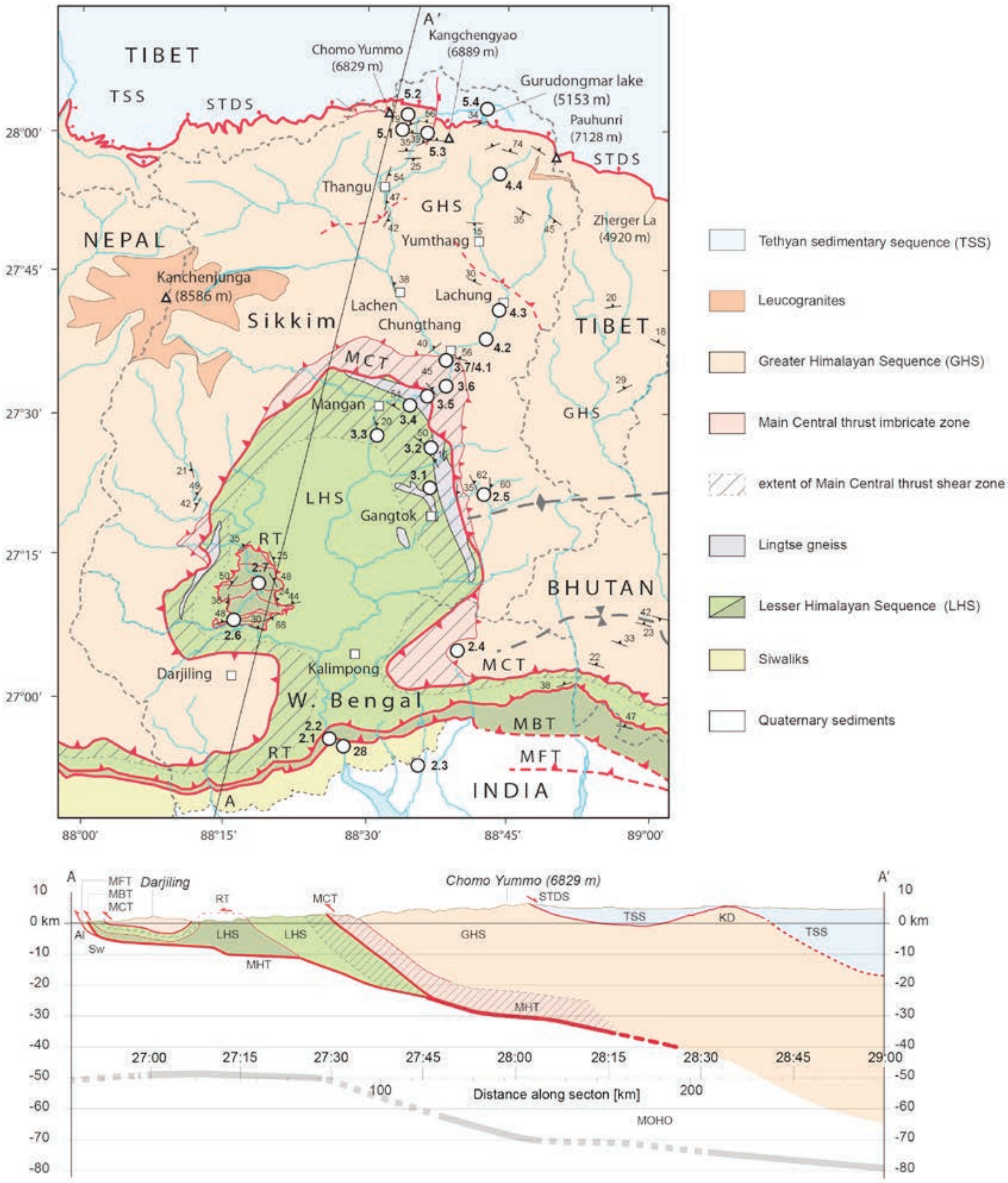

Figure 1.1
Geological map of Sikkim and Darjeeling Himalaya. Compiled from: Gansser, (1983), Bhattacharyya and Mitra (2009), Long et al. (2011b), Kellett et al. (2013), Mottram et al. (2014). All stop locations for the field guide are indicated. STDS-South Tibetan detachment system, MCT-Main Central thrust, RT-Ramgarh thrust, MBT-Main Boundary thrust, MFT-Main Frontal thrust.

that illustrate the geology and particularly the structures of the region. The transect be gins at the southern orogenic front and travels north across the youngest structures of the Himalayan wedge, including neotectonic features and the Main Boundary thrust (Section 2). Above the Main Boundary thrust, the Lesser Himalayan sequence is stacked into a tight duplex, exposed along the Rangit River in the "Rangit window". The guide then works northwards, visiting outcrops within the high strain zone of the MCT (Section 3). The Greater Himalayan sequence, sitting in the hanging wall of the MCT, is described in Section 4. The guide finishes in the north with one of the oldest structures of the Sikkim-Darjiling Himalaya, the STDS (Section 5). For introduction to the geology of the Himalaya particular to the Sikkim-Darjiling region beyond those at the beginning of each section, see Mukul (2000; 2010), Kellett et al. (2013), and Mottram et al. (2014).

Elevation in this map region ranges from near sea level within West Bengal to the top of Kangchenjunga, the world's third highest peak at 8586 m, and the many roadways climbing through its hills permit relatively quick travel from low, humid, leech-friendly valley floors (worst leech infested areas are around 1500-3000 m in elevation!) to cold, high altitude, exposed regions. Those who have worked or travelled in drier Himalayan regions such as central Nepal may notice that Sikkim is a wet climate (Bookhagen and Burbank, 2010). As Sikkim remains a seismically active region, the several dams and exposed roadway leave the region vulnerable to earthquakes such as the magnitude 6.9 earthquake on 18 September, 2011, ~ 68 km NW of Sikkim's capital Gangtok.

2 FRONTAL DARJILING-SIKKIM HIMALAYAN WEDGE

The Indian plate collided with the Eurasian plate along a large-scale (1000s of km), frontal, arc-shaped Himalayan boundary (Bendick and Bilham, 2001; Macedo and Marshak, 1999; Marshak, 2004). However, smaller scale sinuosity (100s of km) of the Himalayan mountain belt exists both in the Himalayan front as well as its hinterland (Fig 2.1). The sinuosity of the Himalayan front has been traditionally recognized in the western Himalaya as salients and recesses (e.g. Dehradun recess/re-entrant, Nahan salient and Kangra recess/re-entrant) (e.g. Powers et al., 1998) (Fig 2.1) and more recently, in the eastern Himalaya as well (e.g. Dharan salient, Gorubathan recess; Mukul, 2010) (Fig 2.1). The salient-recess transitions are typically recognized to be lateral or oblique ramps (Dubey et al., 2001; Yin, 2006) on the Main Himalayan thrust or tear faults (Mukul, 2010; Sahoo et al., 2000). Himalayan salients, recesses and associated transitional structures have impact on the variation of the deformation kinematics along the length of the Himalayan arc over space and time.

The Darjiling-Sikkim Himalaya spills over a salient-recess pair; the Gorubathan recess and the Dharan salient (Mukul, 2010; Fig 2.2). The salient-recess transition is characterized by a sinistral tear fault named the Gish Transverse Fault (GTF).

The geometry of the Himalayan orogen is wedge-shaped (Fig 2.3); the base of this wedge is defined by a north-dipping decollement named the Main Himalayan thrust (MHT) (Schelling and Arita, 1991; Nelson et al., 1996). Several east-west trending and south-vergent shear zones and thrust faults such as the Main Central thrust (MCT), Ramgarh thrust (RT) and Main Boundary thrust (MBT) sole with the MHT (Srivastava and Mitra, 1994; Nelson et al., 1996); the near- surface expression of the MHT is the MFT (Gansser, 1983; Lavé, and Avouac, 2001). The Himalayan wedge is defined as the region between the Indus-Tsangpo suture to the north and the Indo-Gangetic Himalayan foreland to the south. The Darjiling-S ikkim-Tibet (DaSiT) Himalayan wedge is characterized by two "dominant" structures that are most likely to have built taper in the wedge and driven the wedge forward into the foreland. The Darjiling-S ikkim Himalaya are characterized by the Lesser Himalayan duplex (LHD) (Fig 2.3) that has been recognized as a prominent structure involving the Daling, Buxa and the Gondwana units through much of the Lesser Himalaya (Bhattacharyya and Mitra, 2009; Mitra et al., 2010; Mukul, 2010). The Daling horses related to the LHD are exposed in the Tista Half window (THW) (Fig 2.3) and the Gondwana horses are exposed in the Rangit Window. The roof thrust of the former is the MCT while the roof thrust of the latter is the Ramgarh thrust; the basal thrust being the MHT-MFT.

Seismicity in the Darjiling-Sikkim Himalaya

The seismicity patterns in the Himalaya have been well established for decades (Ni and Barazangi, 1984) wherein the bulk of the Himalaya (with the exception of Darjiling-Sikkim and Bhutan Himalaya) has been dominated by thrust earthquakes. Typically, the clustering of epicentres has been recognized to occur between the surface traces of the MCT and the MBT and have been typically attributed to activity along MHT (Pandey et al., 1999). However, great earthquakes have not been recorded in the recent or historic past from the Darjiling-S ikkim and Bhutan Himalaya. Given this, it has been postulated that a great earthquake of magnitude > 7 is practically imminent in the region (Bilham et al., 2001). The observed seismicity in the DSH is dominated by frequent moderate earthquakes. The strongest concentration of epicentres was found to occur between the surface traces of the MBT and MCT between the latitudes 27 º N and 27.5ºN indicating that the Tista half-window records majority of the earthquakes in the area (Pandey et al., 1999; De and Kayal, 2004; Mishra et al., 2010; Kumar et al., 2012) (Fig 2.4). In contrast, eastern Nepal records moderate and microearthquakes along the entire length of the Himalayan wedge (Pandey et al., 1999, de la Torre et al., 2007).

Focal mechanisms of the moderate earthquakes

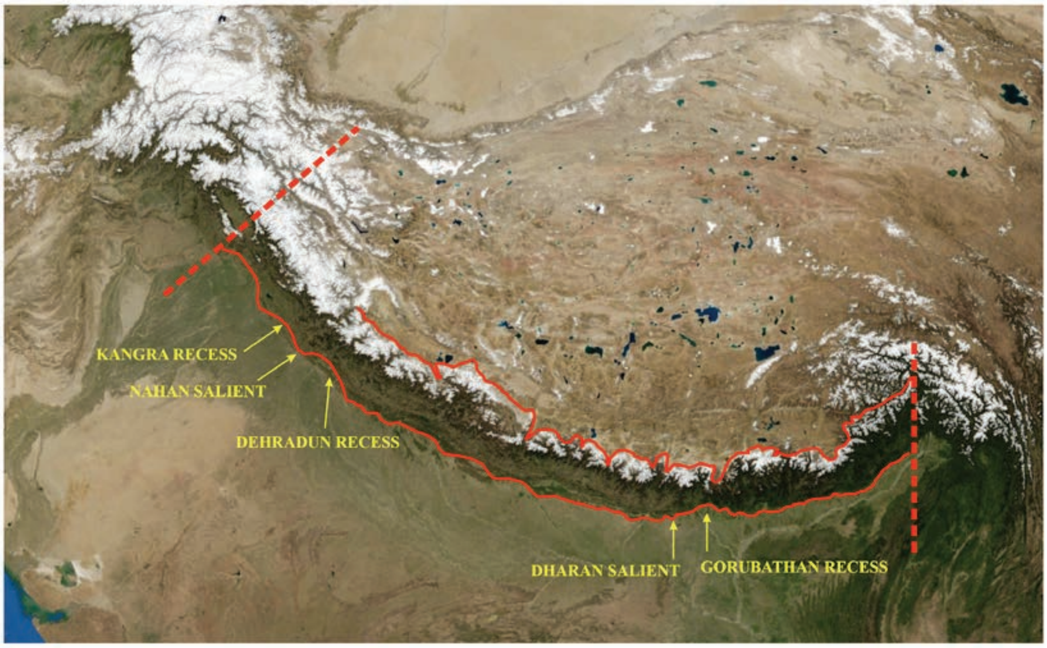

Figure 2.1
The Himalayan arc has a sinuous front at 100s km scale even though it has been recognized as a perfect arc at larger scales (Bendick and Bilham, 2001). The sinuosity is reflected in the formation of salients and recesses that are separated by transition zo nes such as active transverse tear faults. Sinuosity exists in the mountain front as well as in the hinterland as evident in the figure (Landsat-7 Image from http://himalayamountains.com).

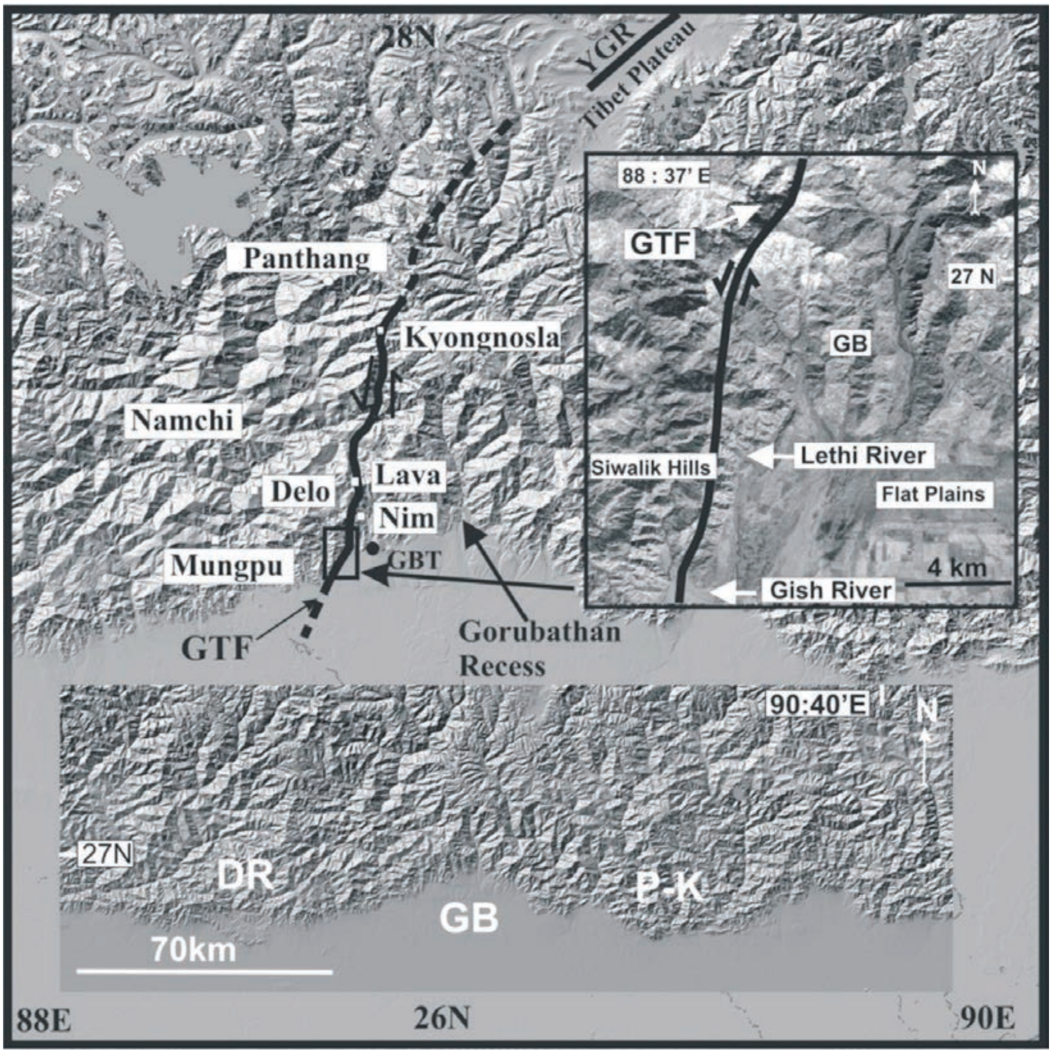

Figure 2.2
SRTM (Shuttle Radar Topography Mission) 90 m based DEM (Digital Elevation Model) of the Darjiling-Sikkim Himalayas showing the Gorubathan (GB) recess, the surface trace of the Gish Transverse Fault (GTF), the Tibet plateau and the Yadong-Gulu Rift (YGR) (from Mukul, 2010). The GTF has a prominent geomorphic expression in the frontal part of the area (right inset) and separates low Siwalik Hills on the west from flat cultivated plains to the east. The GTF has developed in the transition zone between the Dharan salient (DR) and the Gorubathan recess (GB). The Gorubathan recess is located between Dharan salient and the Phuntsoling-Kalikhola (P-K) salient in Bhutan (bottom inset).

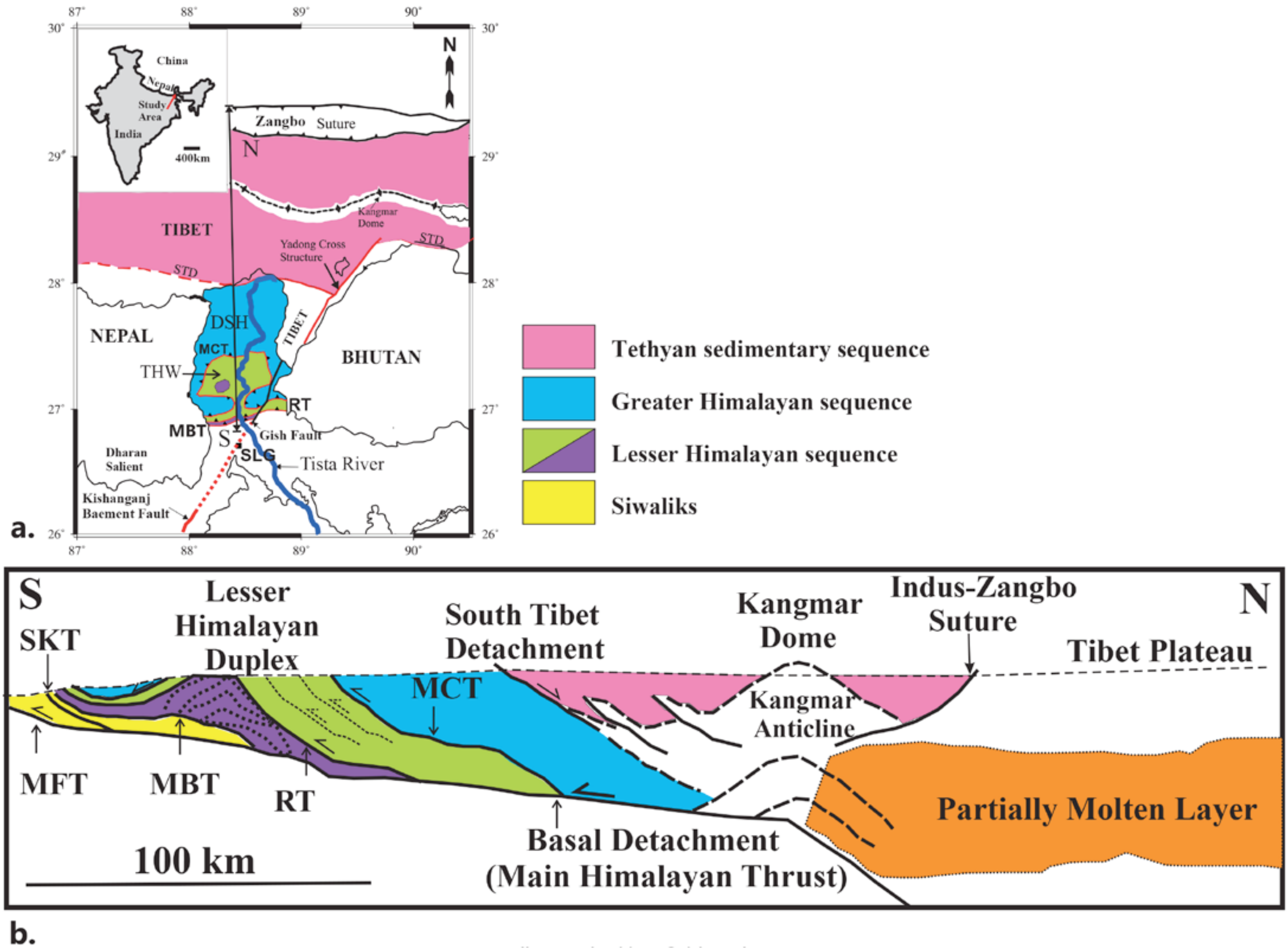

Figure 2.3

Plan and sectional view of the Darjiling-S ikkim-Tibet Himalayan wedge. DSH- Darjiling-Sikkim Himalaya; SKT-South Kalijhora Thrust; MCT-Main Central Thrust; RT- Ramgarh Thrust; MBT-Main Boundary Thrust; MFT-Main Frontal Thrust; THW-Tista Half Window; STD-South Tibet Detachment; SLG-Siliguri.

in the DSH indicate both thrust and strike-slip earthquakes (Fig 2.5). Prominent thrust earthquakes in the region include the 14 February, 2006 Sikkim earthquake of magnitude 5.3 (Mw) (Raju et al. 2007; Hazarika et al, 2010) as well as the 6.1 (Mw), 12 January, 1965 earthquake near eastern Nepal (Baranowski, 1984). However, moderate strike-slip earthquakes abound in the region (Ni and Barazangi, 1984; de la Torre et al., 2007; Raju et al., 2007). Significant strike-slip earthquakes include the November 19, 1980 Sikkim earthquake of Mb 6.2 (Ekstrom, 1987), February 12, 2001 of Mw 4.8, 20 May 2007, Mw 4.9 (de la Torre et al., 2007), and the 18 September, 2011 magnitude Mw 6.9 earthquake close to the Nepal–Sikkim border (Rajendran et al., 2011; Kayal et al., 2011; Kumar et al., 2012). This clearly indicates that both strike-slip and thrust seismotectonics are operational in the Darjiling- Sikkim and Bhutan Himalaya (e.g. Drukpa et al., 2006).

The Main Boundary thrust (MBT 1-N 26.92475˚, E 88.44895˚; MBT 2-N 26.92502˚, E 88.45403˚)

The Main Boundary thrust is best exposed in the Kalijhora village area of the Darjiling Himalaya (Fig. 1.1, Table 2.1). The rocks are exposed in the Kalijhora and Tista river sections. Some of the outcrops described below have been destroyed in the development activities in the area related to

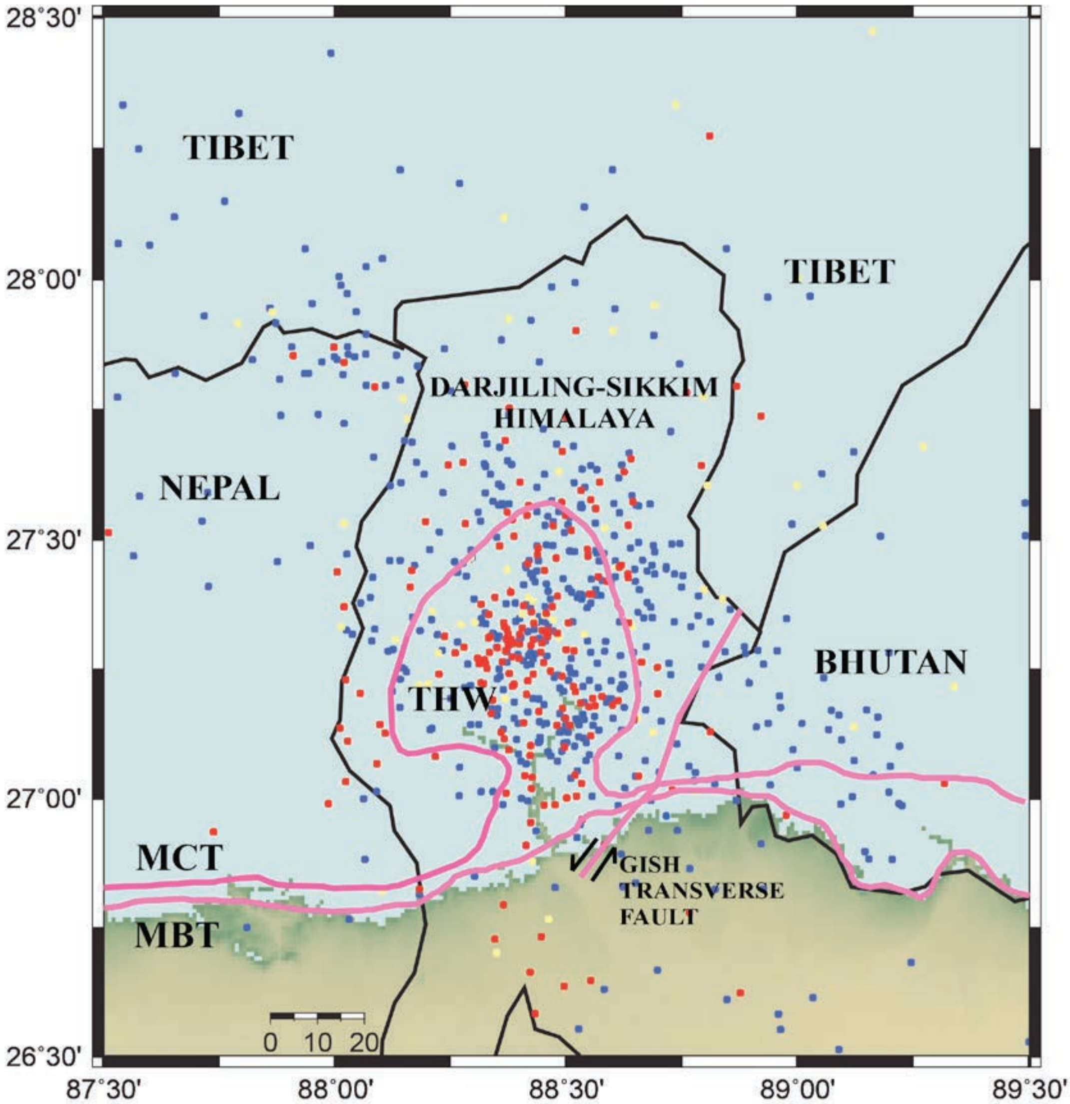

Figure 2.4
Distribution of seismicity in the Darjiling-Sikkim Himalaya (DSH) (after Mishra et al., 2010). Moderate earthquake distribution is shown as color coded circles (Red <3; Blue 3-4; Yellow >4). The micro-seismicity shows a concentration centered around the Lesser Himalayan Duplex (LHD) in the Tista Half Window (THW) which indicates that the LHD might be an active structure and causing the earthquakes.

Table 2.1
Virtual field trip stops for frontal Darjiling-Sikkim Himalaya wedge.

	Locality	Lat (N)	Long (E)	Description
2.1	MBT 1	26.92475°	88.44895°	Main boundary thrust, upper Kalijhora river
2.2	MBT 2	26.92502°	88.45403°	Main boundary thrust, lower Kalijhora river
2.3	GTF 1	26.87611°	88.60288°	Gish river in Himalayan foreland
2.4	GTF 2	27.08429°	88.66658°	Near Lava town, close to Indo-Bhutan border
2.5	GTF 3	27.36821°	88.71383°	Near Nathu La, Indo-Tibetan border
2.6	LHD 1	27.13328°	88.27953°	Tista half window, Jorethang horse
2.7	LHD 2	27.20002°	88.32634°	Tista half window, Dong horse
2.8	S of Kalijhora village	~26.9177°	~88.4647°	1 km south of Kalijhora village, on National Hwy 32A

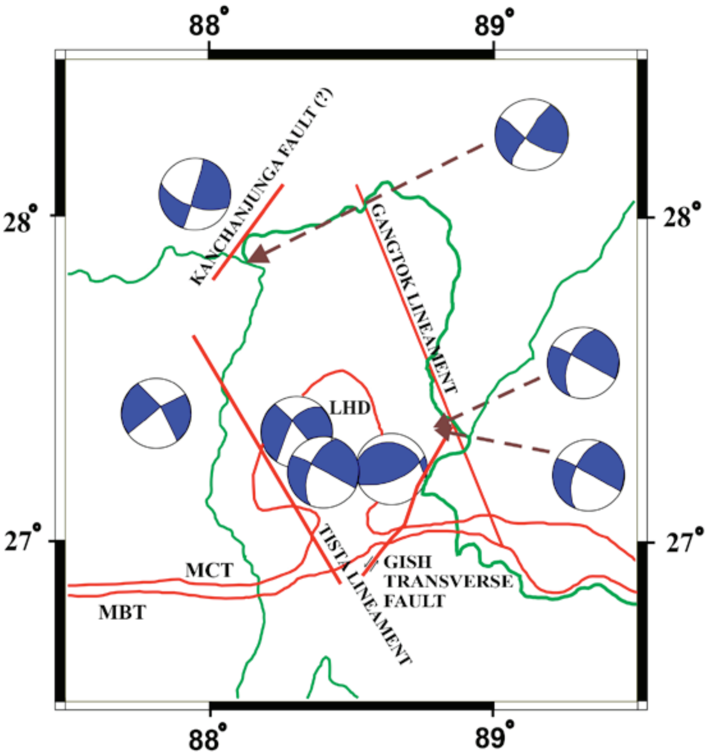

Figure 2.5
Map showing the main focal mechanisms seen in the Darjiling-Sikkim Himalaya. Both moderate thrust and strike-slip earthquakes are seen in the DaSiT wedge which points to the fact that both thrusting and strike-slip faulting is active in the DSH.

the construction of a dam on the River Tista on the MBT fault zone (Figure 2.6).

The Main Boundary thrust carries Gondwanan coarse-grained sandstone and shale over the Lower Siwalik fine-grained sandstones. The fault zone itself has been folded by younger thrusts (Mukul, 2000). At stop 2.1 (MBT 1) the fault zone is characterized by deformed coal and shale that dip to the north (Fig 2.7). Folding of the MBT fault zone is evident from change of dip of the fault zone from northerly to south-westerly as shown in Fig 2.8. Antiformal folding of the MBT fault zone and the hanging wall rocks around a north-easterly plunging fold axis is indicated by the stereoplot. The south dipping limb of the folded MBT fault zone is exposed at stop 2.2 (MBT 2). The exposure represents the inverted south-dipping limb of the folded MBT fault zone. The core of the MBT fault zone is well exposed here and characterized by deformed coal that has undergone flow in the core of the fault zone (Fig 2.9) around Lower Siwalik sandstone clasts in a "mixed" zone.

In the hanging wall, the Gondwana sandstone is brecciated (Fig 2.10) and the beds as well as the cleavage dip moderate to steeply to the south in hanging wall as well as footwall rocks indicating that the entire exposure of the MBT fault zone near MBT 2 is overturned (Fig 2.11). The folding of the MBT fault zone also suggests that the MBT is unlikely to be seismogenically active because a fault can only be folded when it has ceased to be active (Boyer and Elliott, 1 982). Therefore, the seismicity observed in Fig 2.4 is, in all probability, not related to the MBT in the Darjiling Himalaya.

The Gish Transverse fault

(GTF 1-N 26.87611˚, E 88.60288˚; GTF 2-N 27.08429˚, E 88.66658˚; GTF-3 N 27.36821˚, E 88.71383˚)

The Gish Transverse fault (GTF) is a transitional structure that has developed between the Gorubathan Recess and the Dharan salient (Fig 2.2). The GTF has been mapped from the Gish River exit in the foothills (stop 2.3, GTF 1) to the Indo-Tibetan border near Nathu La (stop 2.5, GTF 3) (Fig 2.12; Table 2.1). With an eastward step the fault continues in the western Bhutan as Lingshi fault (Gansser, 1983). The fault near the Gish River exit has a topographic expression and separates low Siwalik hills to the west from alluvial flat land characterized by Quaternary surfaces (Nakata, 1989) (Fig 2.13); Siwalik rocks have not been exposed at all in the Gorubathan recess.

The core of the GTZ is characterized by fine-grained incohesive fault gouge, much of which has turned to soil. The fault zone is recognized by the presence of cemented fault gouge as well as island-channel structures. The islands consist of less deformed rocks and are surrounded by more deformed and grain-size reduced channels that swivel or flow around the islands (Newman and Mitra, 1994) (Fig 2.14). Brittle overprinting of earlier ductile structures such as schistosity is also seen (Fig 2.15a). These observations indicate that the GTZ is an elastico-frictional fault that was active in near-surface conditions. The GTZ fault and fault damage zone are characterized by widespread sub-vertical fracturing (Fig 2.15b) trending approximately N-S following the overall trend of the GTZ.

Lesser Himalayan duplex (LHD 1- N 27.13328˚, E 88.27953˚; LHD 2- N 27.20002˚, E 88.32634˚)

The Lesser Himalayan duplex (LHD) was first

Figure 2.6
Google Earth Imagery (tilted) showing the location of Main Boundary Thrust Fault zone outcrops near the join of Kalijhora with Tista. The view is oriented N-S with N at the right hand side of the image.

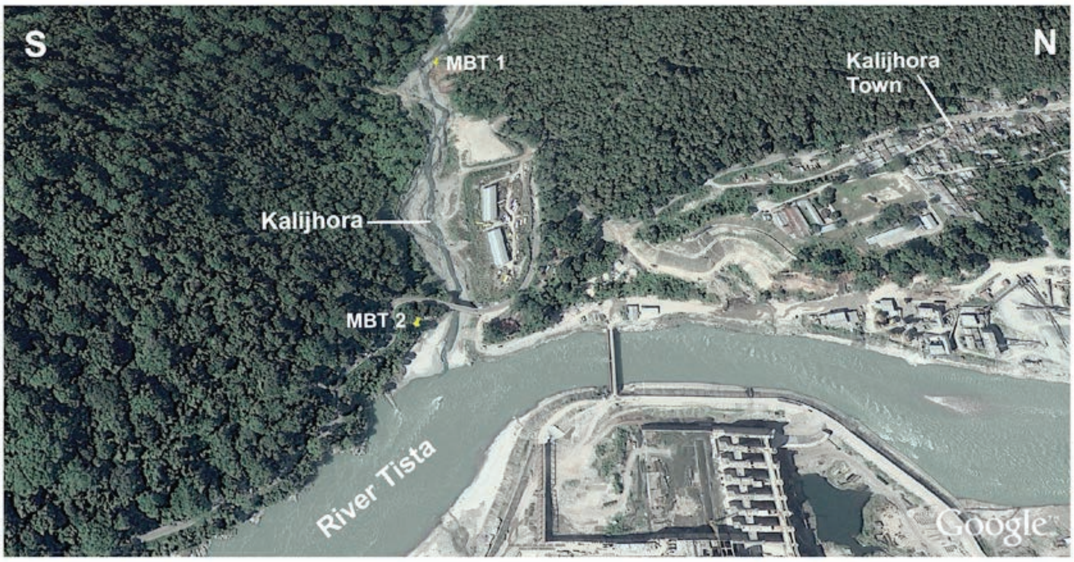

Figure 2.7
Main Boundary Thrust exposure at location MBT 1. Equal area stereoplot of poles to predominantly NW dipping bedding (•) and cleavage ( ) in the shale and sandstone of the Main Boundary Fault zone seen in Fig 2.6. Cleavage is observed to be sub-parallel to bedding in the fault zone.

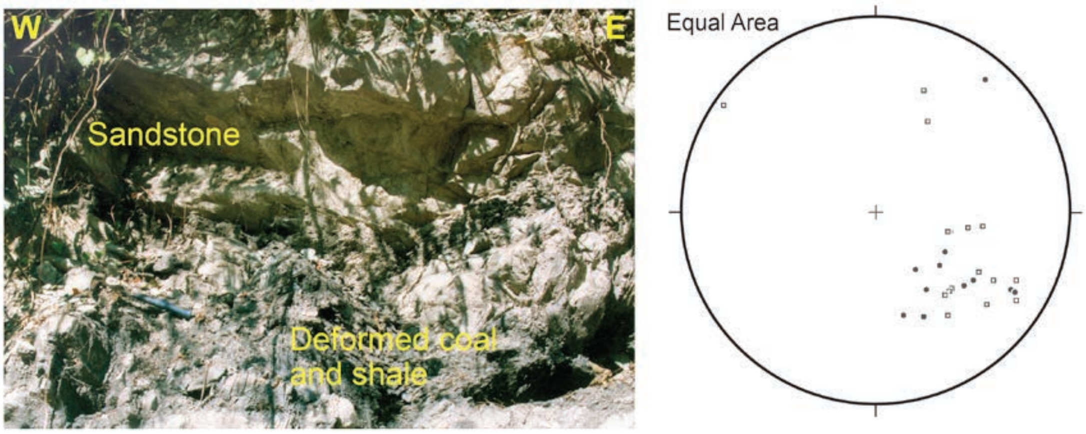

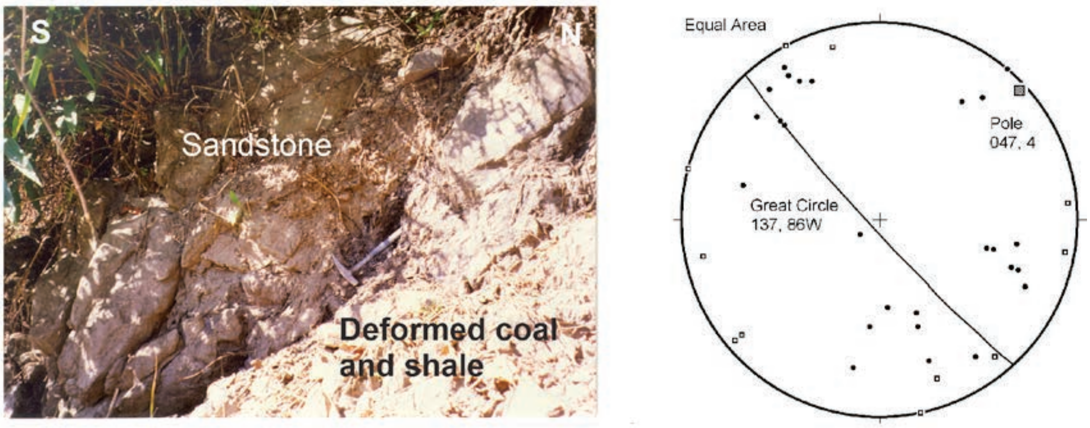

Figure 2.8
Main Boundary Thrust exposure at location MBT 1. Evidence of folding of the Main Boundary Thrust fault zone along with the hanging wall Gondwana sandstones. (a) The fault contact (seen by the location of the hammer) and the hanging wall Geabdat sandstones dip southerly in this photograph as opposed to their north-west dip seen in Figure 2.6. Equal area stereoplot of poles to bedding (•) and cleavage ( ) in the hanging wall of the MBT in the Gondwana Geabdat sandstone along the northern bank of the Kalijhora section.

Figure 2.9
The core of the MBT fault zone and the contact between the Gondwana deformed coal and Lower Siwalik sandstones is a "mixed" zone and seen in the picture above. The sandstone occurs as clasts in a matrix of fine - grained deformed coal that "flows" around the sandstone clasts. Sandstone clasts show brittle deformation and extensive fracturing.

Figure 2.10
Exposure of the Gondwana sandstone in the MBT fault zone at location MBT 2. Fine-grained cemented breccia zone along the boundary of the MBT fault zone rocks and the hanging wall Geabdat sandstones observed along the southern bank of the Kali-jhora stream section close to its junction with River Tista. The fault plane defined by the breccia is sub- parallel to the plane of the paper and the pen (scale) sits on it. The brecciated zone dips to the southeast indicating that the MBT fault zone is probably folded into an antiform-synform pair in which the synform is overturned.

postulated from a balanced cross-section in the Kumaon-Garhwal Indian Himalaya below the present day level of erosion (Srivastava and Mitra, 1994). The LHD has been subsequently mapped at the present day level of erosion in Nepal (DeCelles et al., 1998), Bhutan (McQuarrie et al., 2008) and Sikkim (Bhattacharyya and Mitra, 2009; Mitra et al., 2010). The LHD is a hinterland-d ipping duplex in Kumaon-Garhwal, central Nepal as well as in Bhutan. In Sikkim, the LHD is a complex structure (Fig 2.16). The frontal horses of the structure are foreland-dipping, the middle horses form an antiformal stack, and the rear horses are hinterland-dipping (Bhattacharyya and Mitra, 2009; Mitra et al., 2010).

The large-scale geometry of the LHD is difficult to illustrate in a field guide. However, outcrop scale structures can be observed. A foreland-dipping horse (stop 2.6, LHD 1) can be observed in the Jorethang horse (Table 2.1). A sandstone-shale-coal Gondwana sequence is exposed here. The bedding dips steeply to the south and is near vertical (Fig. 2.17). The coal seams and shale have undergone brittle deformation and form centimetre- to metre-scale fault zones (Fig. 2.17). Farther north, the LHD contains horses that dip to the north, describing a hinterland-dipping duplex (stop 2.7, LHD 2). Outcrop-scale horses and fault zones are also seen within the large horses; these also dip to the north (Fig. 2.18) (Mukul, 2010). The LHD, in all probability, is an active structure in the Darjiling-S ikkim Himalaya (Figs. 2.4, 2.5) as very pronounced clusters of earthquake epicentres are located within the trace of the LHD. The LHD, kinematically, is a "dominant" structure that has driven the Darjiling-S ikkim Himalayan fold-and-thrust belt southward into its foreland (Mukul, 2010).

Neotectonics in the frontal Darjiling-Sikkim Himalaya (~N 26.9177˚, ~E 88.4647˚)

The Darjiling-Sikkim Himalaya is characterized by a frontal imbricate zone in the footwall of the MBT that repeats the Siwalik section multiple times (Mukul, 2000; Mukul et al., 2007; Kundu et al., 2011; 2012). Out-of-sequence thrusts are observed within this imbricate zone on surface-breaking faults north of the MFT in the Darjiling sub-Himalaya. The Tista River responded to this deformation by migrating 150 m eastward

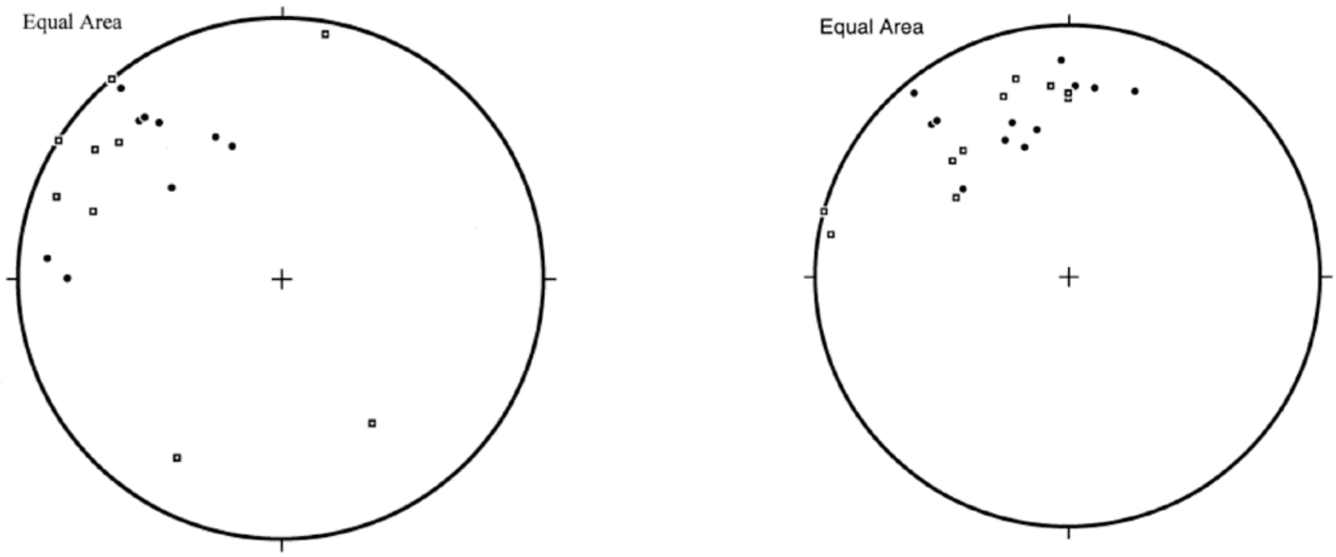

Figure 2.11
(a) Equal area stereoplot of poles to bedding (•) and cleavage ( ) within the MBT fault zone near the junction of Kalijhora stream and Tista River (Location MBT 2). The cleavage and bedding within the fault zone dip south-easterly and are sub-parallel. (b) Equal area stereoplot of poles to bedding (•) and cleavage ( ) in the hanging-wall Gondwana sandstones of the MBT fault zone. Both the bedding and the cleavage within the fault zone dip moderately to the southeast near the junction between Kalijhora stream and Tista River and are sub -parallel

(average rate ~ 13 mm/ yr) and by incising 48 m vertically (average rate ~ 4.4 mm/ yr), creating unpaired, disjointed strath terraces between 11.3 – 1.3 ka and 1.4 – 0.3 ka (Mukul et al., 2007). The site of this out-of-sequence neotectonics is about 1 km south of Kalijhora village along the National Highway 32A in Darjiling-Himalaya (stop 2.8 of Table 2.1, Fig 2.19). Out-of sequence splays that display well-formed fault gouge are seen in the Tista river section (Fig 2.20); raised strath fluvial terraces are seen to the north and in the hanging wall of these splays. It is interpreted that these terraces are neotectonic in origin as they occur only in the immediate hanging-wall of the out-of-sequence splays and are associated with them both in space and time.

Out-of-sequence deformation has been postulated as a mechanism to build taper in a sub-critical Coulomb wedge (DeCelles and Mitra, 1995) which, therefore, suggests that the foreland fold-and-thrust belt of Darjiling-S ikkim Himalaya is deforming internally and building taper to attain criticality (Mukul et al., 2007).

3 MAIN CENTRAL THRUST

The Main Central thrust (MCT) is a major structure in the Himalayan orogen that has accommodated a substantial amount of the India-Asia convergence (Gansser, 1964; Schelling and Arita 1991). The MCT plays a pivotal role in tectonic models such as channel flow (Beaumont et al. 2001) and wedge extrusion (Kohn 2008). Despite its importance in understanding of geological processes in the Himalayas, its location is in dispute in many transects (Searle et al. 2008) and poorly known in some areas. The MCT is one of the most controversial structures in the Himalaya, due to the divergent criteria used to define the thrust, differences in the methods and approaches of those who study it, and variations in the thrust along the length of the Himalaya.

The MCT separates the Greater Himalayan sequence (GHS) in the hanging wall from the Lesser Himalayan sequence (LHS) in the footwall. Along the entire orogen the MCT is a ductile shear zone, where the precise location is often unclear due to the diffuse nature of the deformation. As there is a difference in the provenance of the rocks either side of the MCT, many recent studies, working in areas where the geological criteria are ambiguous, have used geochemistry as a complementary tool to identify and investigate the tectono-stratigraphic break across the MCT. It has been shown that the LHS is a Palaeoproterozoic sequence with an εNd(0) signature of -20 to - 25, which has been intruded by ca. 1.8 Ga granites, whereas the GHS

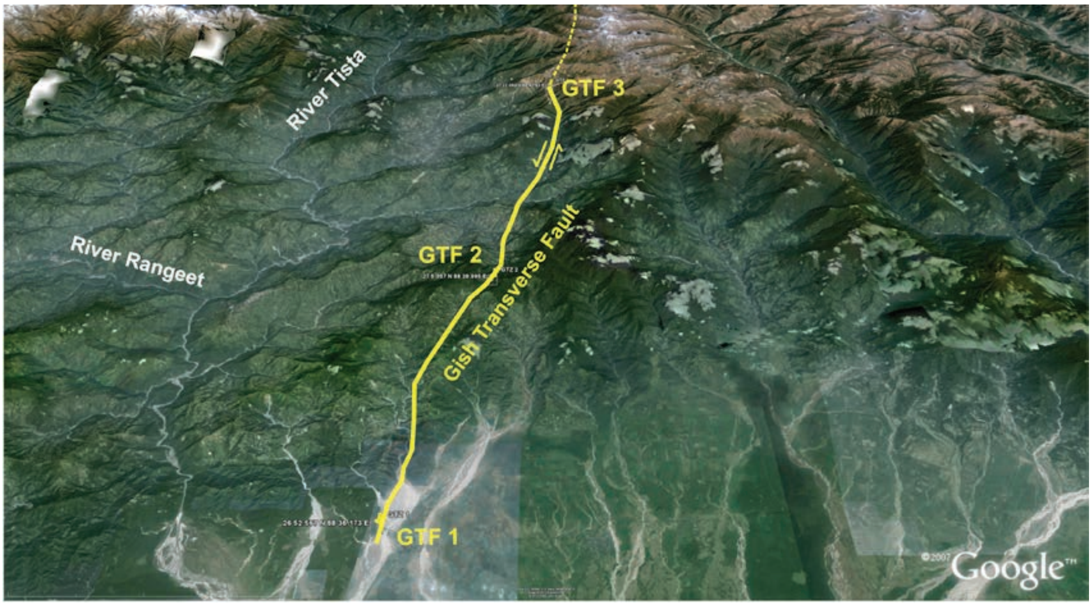

Figure 2.12
Google Earth Imagery (tilted) showing the location of the surface trace of the Gish Transverse Fault between the Himalayan foreland (GTF 1) and the Indo-Tibetan border (GTF 3) near Nathula Pass.

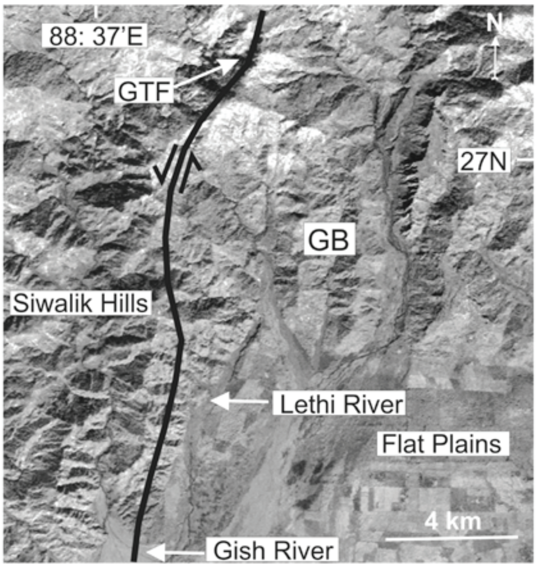

Figure 2.13
Surface trace of the GTF near GTF 1 (Mukul, 2010). Siwalik Hills are separated from flat plains in the Gorubathan recess (GB) by the GTF in the satellite imagery of the foothills of the Darjiling Himalaya. Geomorphic expression of the GTF is best preserved in the foothills

is a younger, Neoproterozoic-Ediacaran (and possibly Palaeozoic) sequence, characterised by an εNd(0) signature of -15 to -20 indicative of younger source regions, typically intruded by younger, Cambro-Ordovician and subordinate Neoproterozoic (ca. 830 Ma) granites. It is therefore possible to use isotope geochemistry to find the protolith boundary between the LHS and GHS where structural criteria are unclear (Parrish and Hodges 1996; Ahmad et al. 2000; Robinson et al. 2001; Martin et al. 2005; Richards et al. 2005; Richards et al. 2006; Imayama and Arita 2008; Tobgay et al. 2010; Gehrels et al. 2011; Long et al. 2011a; Martin et al. 2011; McQuarrie et al. 2013; Webb et al. 2013).

Sikkim presents an ideal location to studying the Main Central Thrust due to the nearly-unique exposure of the MCT. The thrust has been folded due to a duplex in the LHS rocks beneath the Ramgarh thrust (Bhattacharyya and Mitra, 2009), forming the Tista dome and one of the largest re-entrants of the MCT in the Himalaya (Fig. 1.1). In the Sikkim Himalaya, the MCT separates the Greater Himalayan Sequence, which comprises gneisses, migmatites, calc-silicates and leucogranites, from the greenschist- facies Lesser Himalayan sequence metasedimentary rocks. The transition between these two lithotectonic units forms a several kilometre thick zone of inverted Barrovian metamorphism (Mohan et al., 1989) and penetrative ductile shear. This has often led authors to refer to the MCT as the Main Central Thrust Zone [MCTZ] (Goswami 2005; Gupta et al. 2010), with two bounding thrusts either side of this shear zone (Catlos et al. 2004; Dubey et al., 2005; Bhattacharyya and Mitra 2009; 2011). This zone consists of pelitic schist, psammite, quartzite, calc-silicate and orthogneiss (locally known as the Lingtse gneiss; Paul et al., 1982), which range from chlorite- to sillimanite-grade metamorphism. Recent work in Sikkim has demonstrated that what has traditionally been mapped as the 'MCT zone' is

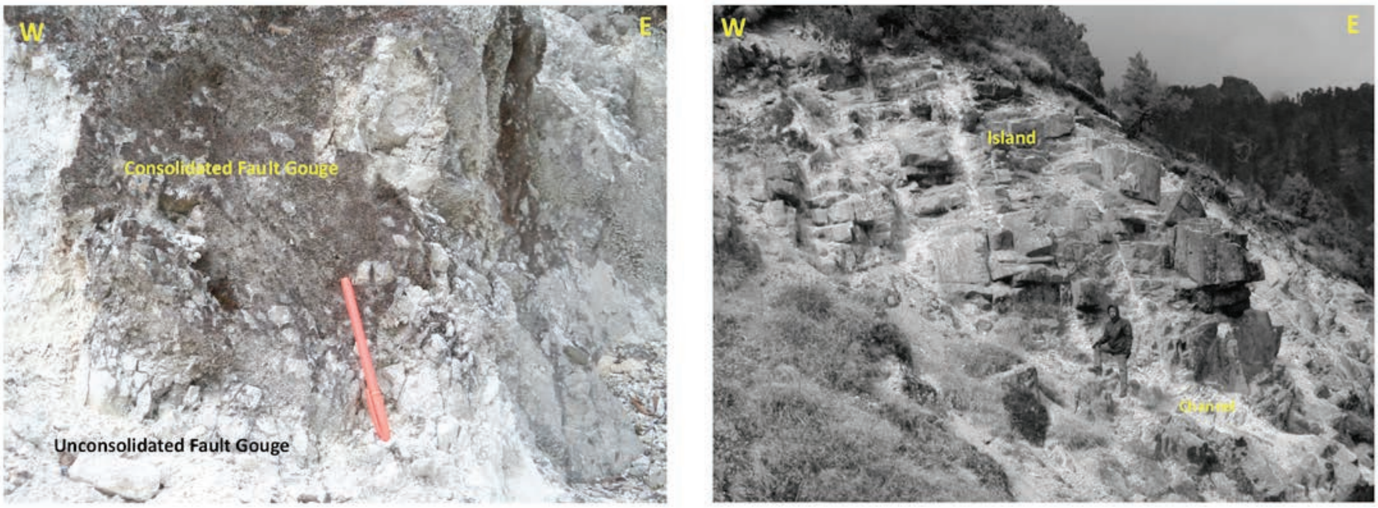

Figure 2.14
(a) Consolidated and unconsolidated fault gouge from the Gish Transverse Fault near GTF 2. Consolidated gouge typically form islands within a groundmass of unconsolidated fine grained gouge near the center of the GTF fault zone (left). (b) Steeply-dipping bedding surrounded by fine-grained unconsolidated fault gouge describing an overall island-channel geometry near GTF 3 (right).

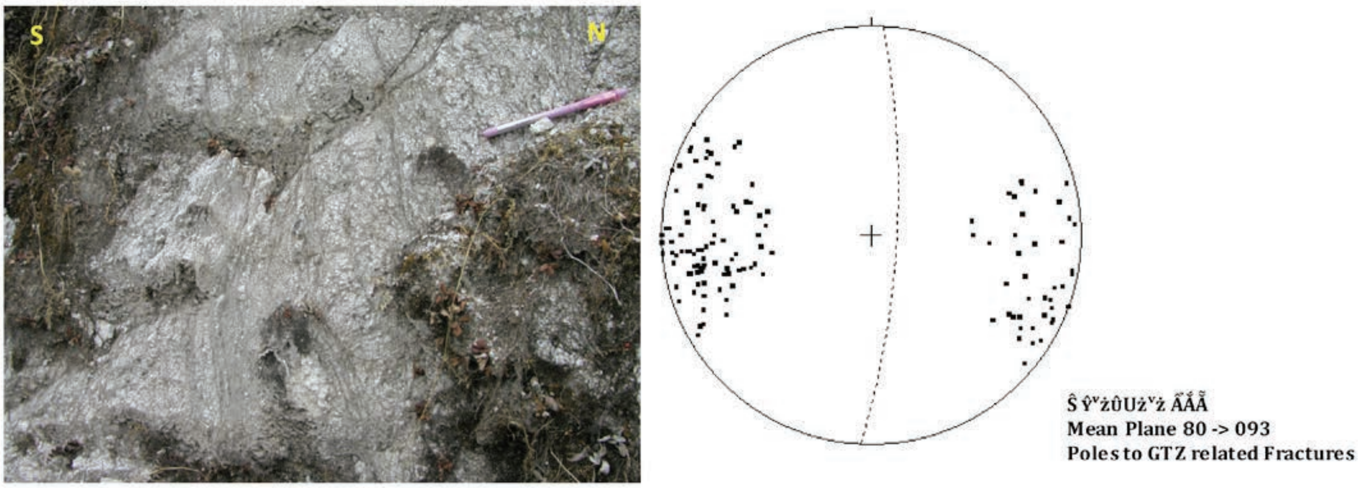

Figure 2.15
(a) Relict schistosity is seen overprinted by brittle structures in gneiss in the GTF fault zone near GTF 3. (b) Equal area plot of pole to GTZ related fractures in the fault damage zone indicating that the GTF is a transverse, steep, east-dipping, sinistral fault.

primarily comprised of Lesser Himalayan provenance rocks, with the MCT protolith boundary located at the top of this zone (Fig. 1.1). The ductile shear associated with the MCT has penetrated down from this protolith boundary into the underlying LHS rocks in a zone of distributed strain. In detail there is a section of imbricated rock in the immediate vicinity of the MCT where rocks of GHS and LHS provenance have become interleaved during ductile thrusting (Fig. 3.1, Mottram et al., 2014).

Due to the nature of the diffuse deformation associated with the MCT, it is not possible to see its characteristic features in a single rock outcrop. The MCT is best viewed in a transect across the zone of ductile deformation formed during thrusting along the MCT. This virtual fieldtrip focuses on a road section through the MCT from Gangtok to Chungthang (Fig. 3.1; Table 3.1). This section cuts through an excellent example of an

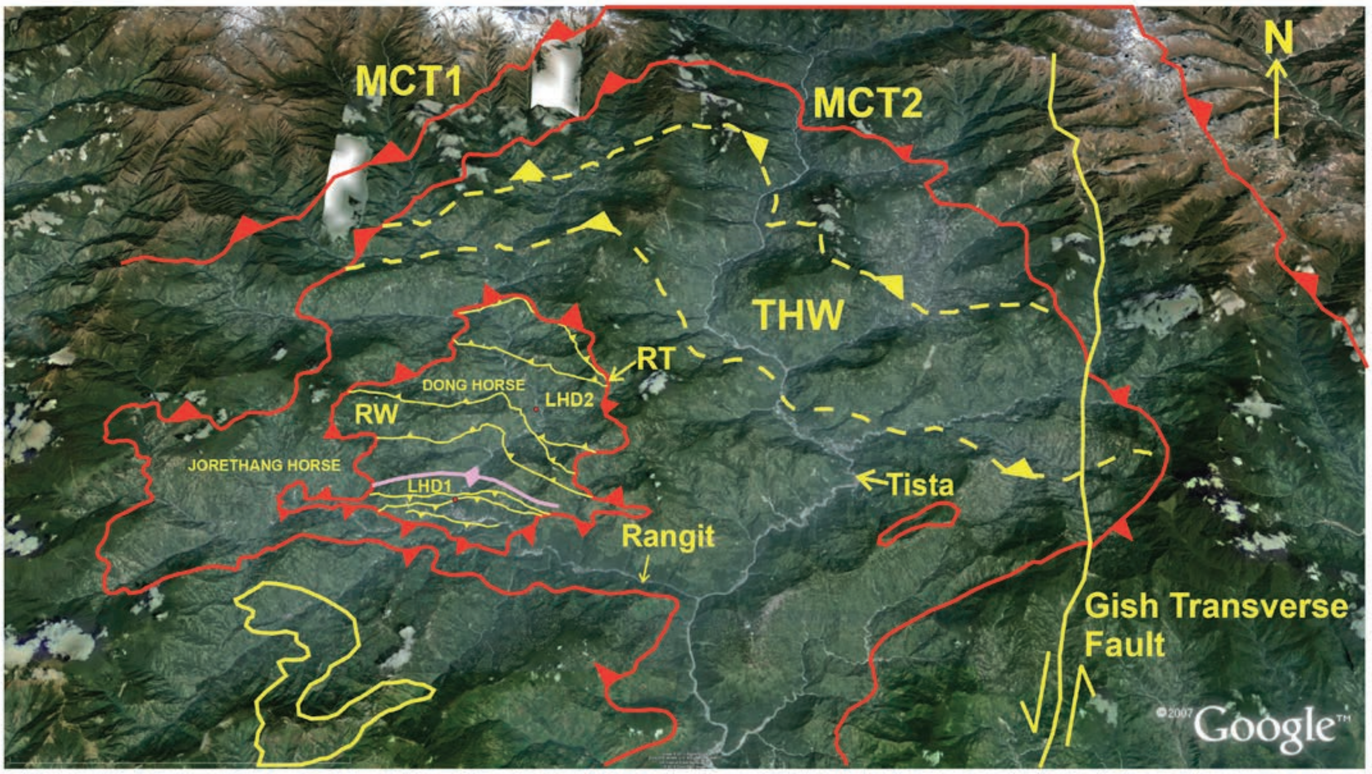

Figure 2.16

The Lesser Himalayan Duplex (LHD) in Sikkim as exposed in the Tista half window (THW) and Rangit Window (RW). The frontal horses of the LHD in the Rangit window dip to the south, the middle horses are folded into an antiformal stack and the rear horses dip to the north defining the most complex LHD geometry mapped in the Himalaya till date (Bhattacharyya and Mitra, 2009; Mitra et al., 2010).

inverted Barrovian metamorphic sequence. The map indicates that as the road travels north from Gangtok to Chungthang, it passes through what is geochemically defined as the Lesser Himalayan Series, ultimately into the Greater Himalayan Series. Towards the top of the zone of deformation there is geochemical evidence for tectonic interleaving in the immediate vicinity of the zone, where a slice of LHS material has been interleaved into GHS rocks (Mottram et al., 2014).

Tashi viewpoint, Gangtok (N 27.37112˚, E 88.61633˚)

The road cut at Tashi viewpoint exposes a good example of the Sikkim Lingtse gneiss. Throughout the Sikkim Himalaya large bodies of orthogneiss can be found strung out beneath the MCT (Fig. 3.1). The Lingtse gneiss (Paul et al., 1982; Paul et al., 1996) is a sheared granite comprised of quartz, K-feldspar, plagioclase, biotite ± muscovite and garnet. The Lingtse gneiss has been dated by U-Pb zircon geochronology at ca. 1830-1850 Ma, with the outcrop at Tashi viewpoint giving an average 207Pb/206Pb age of 1837 ± 47 Ma (Mottram et al., 2014). These Lesser Himalayan affinity granites can be correlated with other granite gneisses across the Himalaya such as the Ulleri gneiss in Annapurna, the Num orthogneiss from the Arun Valley, the Phaplu augen gneiss from Everest and the Bomdila gneiss in Arunachal (Goswami et al. 2009; Kohn et al., 2010). It has been suggested that these rocks formed during the formation of the supercontinent Columbia (Kohn et al., 2010).

The outcrop at Tashi viewpoint shows clear folding and well-developed stretching lineations (Fig. 3.2). This demonstrates how the Paleoproterozoic Lingtse granites were strongly deformed by movement along the MCT during the Miocene, as shown by N-S mineral lineations, folding and stretched tectonite fabrics throughout the region.

Figure 2.17
The Lesser Himalayan Duplex (LHD) in Sikkim as exposed in the Tista half window (THW) and Rangit Window (RW) near LHD 1 in Fig 2.15. The frontal horses of the LHD in the Rangit window such as the Jorethang Horse dip to the south. Fault zones have developed in the coal and shale formations. (Matin and Mazumdar, 2009; Bhattacharyya and Mitra, 2009; Mitra et al., 2010)

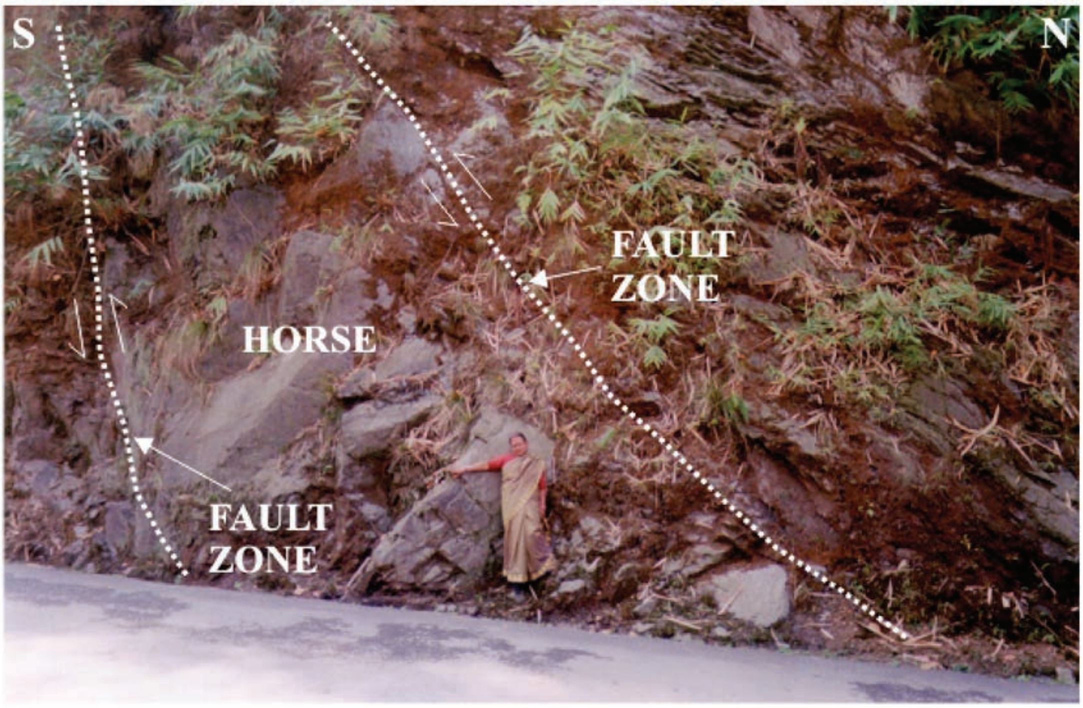

Figure 2.18
The Lesser Himalayan Duplex (LHD) in Sikkim as exposed in the Tista half window (THW) and Rangit Window (RW). The frontal horses of the LHD in the Rangit window dip to the south, the middle horses are folded into an antiformal stack and the rear horses dip to the north defining the most complex LHD geometry mapped in the Himalaya till date (Bhattacharyya and Mitra, 2009; Mitra et al., 2010). A hinterland-dipping outcrop scale horse is seen in the figure near LHD 2 in Fig 2.15

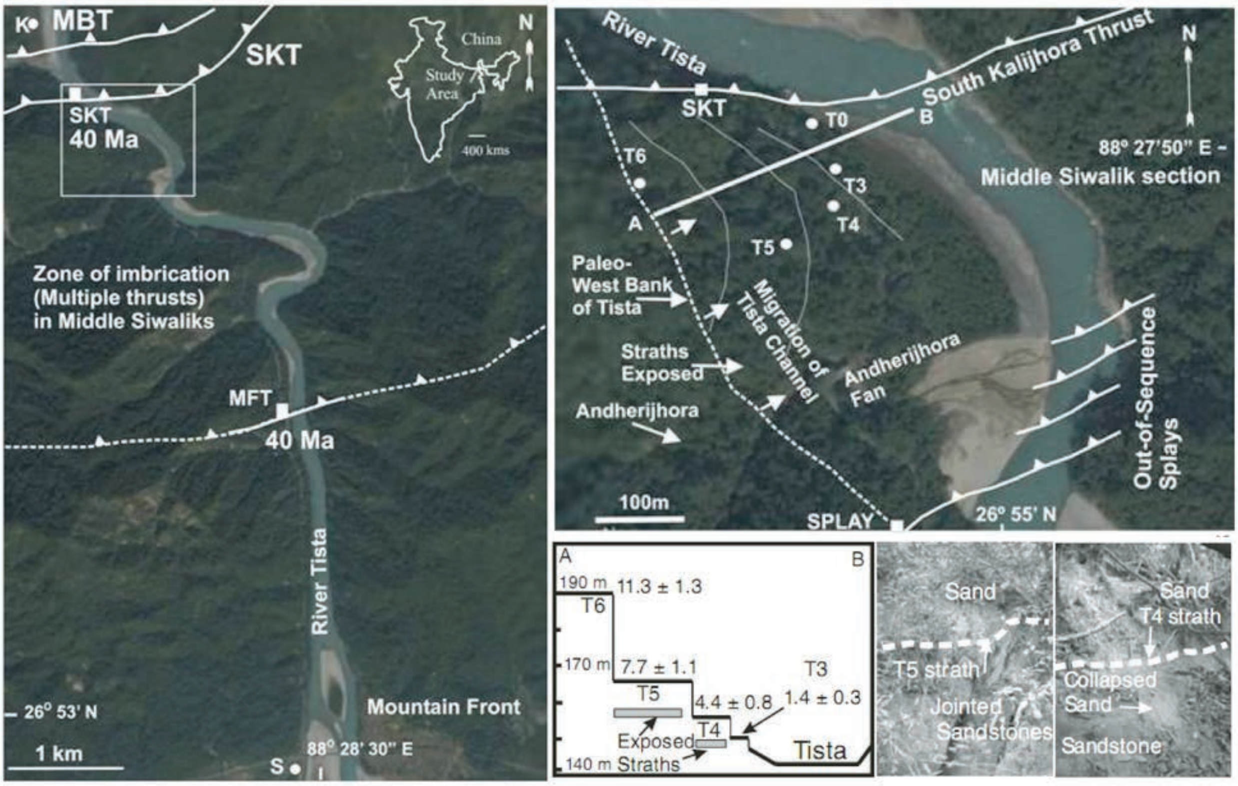

Figure 2.19
Out-of-sequence deformation in the frontal Darjiling-S ikkim Himalaya (Mukul et al., 2007). Sample locations of fault-zone gouge north (South Kalijhora thrust, SKT) and south (Main Frontal thrust, MFT) are shown by white squares. S-Sevak; K-Kalijhora; MBT-Main Boundary thrust. Out-of-sequence splays and Tista terraces (T3- T6). Straths are only exposed in the Andherijhora section, as shown on the imagery on the right (top). White circles indicate sample locations of terraces; white squares indicate fault-zone gouges. T0 is sample location of modern sand. Scaled section of terraces is shown in right (bottom) (along AB). Ages are given in ka. Field photographs show strath surfaces as seen in Andherijhora section.

Figure 2.20
Out-of-sequence imbricate faults (marked by arrows) that repeat Middle Siwalik (Tertiary) sandstone. Fault gouge from the southern-most imbricate was dated to be 20 ka. The fault zones have developed in the shale. The scale bar is 15 m.

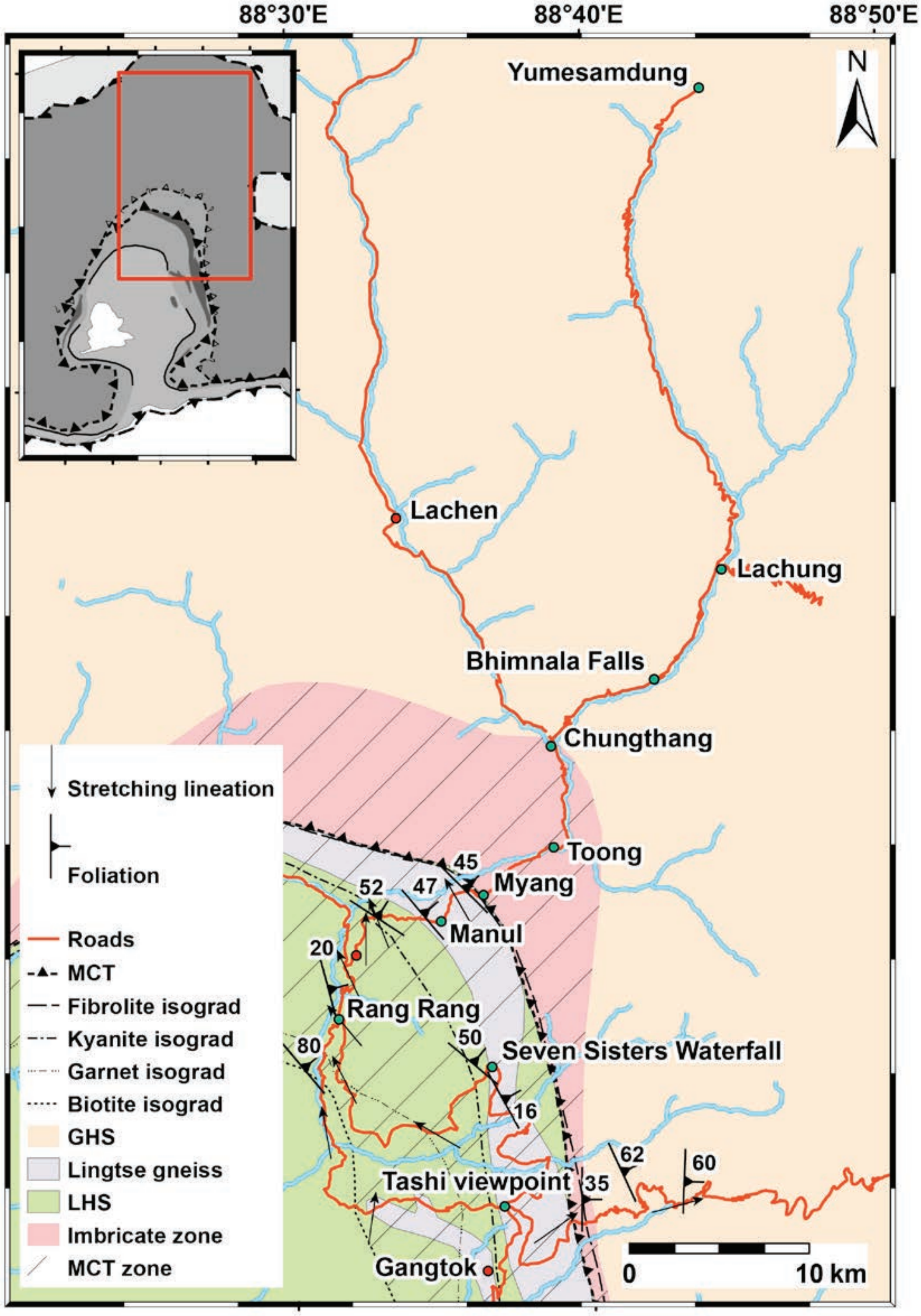

Figure 3.1
Map of Main Central thrust and Greater Himalayan sequence localities in the Gangtok-Mangan section, inset shows location of section in NE of Sikkim. The upper boundary of the MCT high strain zone is positioned at the protolith boundary of Mottram et al. (2014). Metamorphic isograds are shown as dotted and dashed lines. The extent of the zone of deformation associated with the MCT is shown as the hatched zone.

Seven Sisters waterfall (N 27.44115˚, E 88.61030˚)

As the road twists north from the Tashi viewpoint at the outskirts of Gangtok, it travels predominantly through more Lingtse orthogneiss as described at the previous locality. The Seven Sisters waterfall cuts through this extended body of Lingtse gneiss and is similar to location 3.1. Only a few meters from the waterfall, along the road towards Mangan, there is an inferred contact between the Lingtse gneiss and the surrounding schists of the MCT zone. Although it has been suggested that there is a thrust contact between the Lingtse gneiss and surrounding 'country rock' (Bhattacharyya and Mitra 2011), shearing associated with the MCT, along with the poor exposure, largely obscures the contact between these rocks which is mainly considered to be an intrusive relationship (Dasgupta et al., 2009; Mottram et al., 2014). The Daling schists which outcrop at Seven Sisters waterfall are kyanite grade and contain virtually pristine examples of euhedral staurolite and kyanite in the garnet + staurolite + kyanite + biotite + muscovite + quartz + plagioclase assemblage (Figs. 3.3 and 3.4c,d). The schists are strongly sheared and have a well-developed schistose foliation which strikes roughly NW-SE, parallel to the trend of the MCT (Figure 3.1). These rocks experienced metamorphic conditions of ~650 °C and ~8-10 kbar which is equivalent to ~20 km depth in the crust (Mottram, 2014).

Rang Rang (N 27.46597˚, E 88.52455˚)

The next stop on the virtual fieldtrip is Rang Rang. Many new road cuts in this area have exposed a stretch of ~2 km of rock which exhibits key structural features of the rocks in the MCT zone. Firstly, the fine-grained micaceous schist has large, perfectly euhedral garnet porphyroblasts (Fig. 3.5), which formed syn-to-post kinematically during MCT shearing. Secondly, shear bands are clearly formed in the fine micaceous phyllitic schist, demonstrating the top-to-the-south sense of shear that is prevalent throughout the MCT shearing.

The stretch of road between localities 3.3 and 3.4 is a very good example of the inverted Barrovian metamorphic sequence seen as a wide zone beneath the MCT in Sikkim. The road twists in and out of the metamorphic isograds exposing rocks of different metamorphic grade. Between Mangan (close to locality 3.3), Singhik and Manul, there is a series of well-developed mica, garnet-mica, and kyanite-staurolite-garnet mica schist units (Fig. 3.4). These rocks show a strong schistosity striking parallel to the MCT in this area (Fig. 3.1). The dominant MCT deformation is also shown as crenulations (Fig. 3.4a), folds, shear bands and north-south mineral lineations formed along the direction of movement on the MCT. The main micaceous fabric is crenulated at the mm scale. The crenulations are overgrown by syn-metamorp hic garnets and subsequently deformed by shear bands defined by quartz-rich lenses. These fabrics all formed within a ductile regime during a prolonged period of shortening and heating during which the rocks were metamorphosed syn-kinematically (as demonstrated in spiral garnet inclusions in Fig. 3.4b), during Miocene shearing on the MCT zone (Fig. 3.6).

Monazite data from this transect demonstrates how the deformation penetrated downward from the structurally higher levels to the lower grade LHS rocks. The kyanite-staurolite schists at the top structural levels yield monazite ages of ca. 15 to 12 Ma, whereas the lower grade mica schist at the lower structural levels yields ages ca. 12-9 Ma (Mottram, 2014), this is in accord with the previous findings of Miocene slip on the MCT in the Sikkim Himalaya (Catlos et al., 2004). Garnet zoning allows for the prograde and peak metamorphic conditions of metamorphism to be calculated, suggesting that the structurally higher grade rocks experienced conditions of around 550 °C and 8-10 kbar during garnet core formation, while the rims formed during peak metamorphism at around 650-675°C and 8-10 kbar during staurolite and kyanite growth. As some samples contain small amounts of fibrolite, it can be inferred that on the retrograde path, rocks passed into the sillimanite field, suggesting isothermal cooling (Mottram, 2014). Overall the data from the inverted metamorphic zone in the Sikkim Himalaya reveals that rocks were metamorphosed during shearing at mid-crustal conditions. Deformation penetrated downwards from the original photolith boundary into the underlying Lesser Himalayan rocks, which became part of the sheared MCT zone.

Manul (N 27.51440˚, E 88.58273˚)

At Manul, there is a further outcrop of Lingtse

Table 3.1
Virtual field trip stops for Main Central thrust and Greater Himalayan sequence.

	Locality	Lat	Long	Description
3.1	Tashi viewpoint, Gangtok	27.37112	88.61633	Lingtse orthogneiss (1.8 Ga granite)
3.2	Seven Sisters Waterfalls	27.44115	88.61030	Lingtse orthogneiss and kyanite-staurolite schists
3.3	Rang Rang	27.46597	88.52455	Garnet schists with beautiful euhedral garnets and shear bands
3.4	Manul	27.51440	88.58273	Lingtse orthogneiss extremely deformed into L-tectonite fabric
3.5	Myang	27.52737	88.60660	Fibrolite schists, moving into an imbricate/mixed zone of GHS/LHS rocks associated with MCT
3.6	Toong	27.55082	88.64648	Large folded calc-silicate, quartzite and sillimanite schist cliffs
3.7 4.1	Chungthang	27.60157	88.64568	Fresh road cuts through gneisses, pegmatites, melt veins and quartzite. This marks the northern-most boundary of the 'MCT-zone'.
4.2	Bhimnala Falls	27.63433	88.70430	Migmatitic pelitic gneisses displaying ductile folding.
4.3	Lachung	27.68598	88.73853	Pelitic gniesses and orthogniess intrusions
4.4	Yumesamdung	27.93057	88.73407	Sillimanite grade gneisses of the GHS.

Figure 3.2
Lingtse gneiss exposed on the roadcut below Tashi viewpoint. The metamorphosed 1.8 Ga granite is deformed and folded by movement on the MCT.

gneiss that yields an average 207Pb/206Pb age of 1836 ± 26 Ma (Mottram et al., 2014). The reason this outcrop is particularly notable is due to the intense deformation not seen in the Lingtse outcrops further south. Figure 3.7 demonstrates how the 'augen' of the orthogneiss have been strongly stretched into an L-tectonite-type fabric. This locality is a good example of how the strain associated with the MCT deformation is recorded differently depending on the rheology of the rock type. It has been asserted that the location n of the MCT should be based on structural observations and located at the point of highest strain (Searle et al., 2008). This section highlights the difficulty of quantifying strain in the MCT zone and shows why other methods such as geochemical classification are often used to define the location of the MCT.

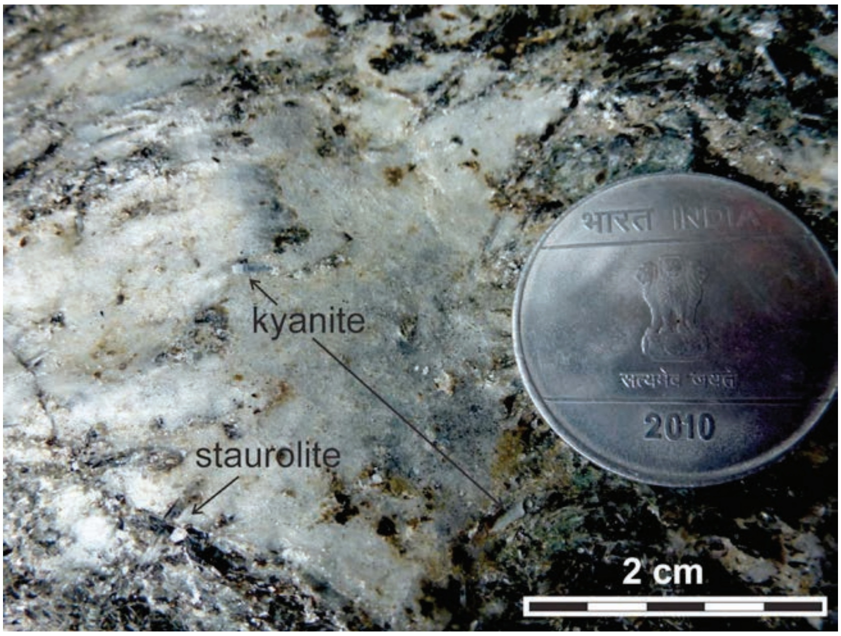

Figure 3.3
Hand specimen photograph of garnet-staurolite-kyanite schist exposed adjacent to the Lingtse gniess at Seven Sisters waterfall.

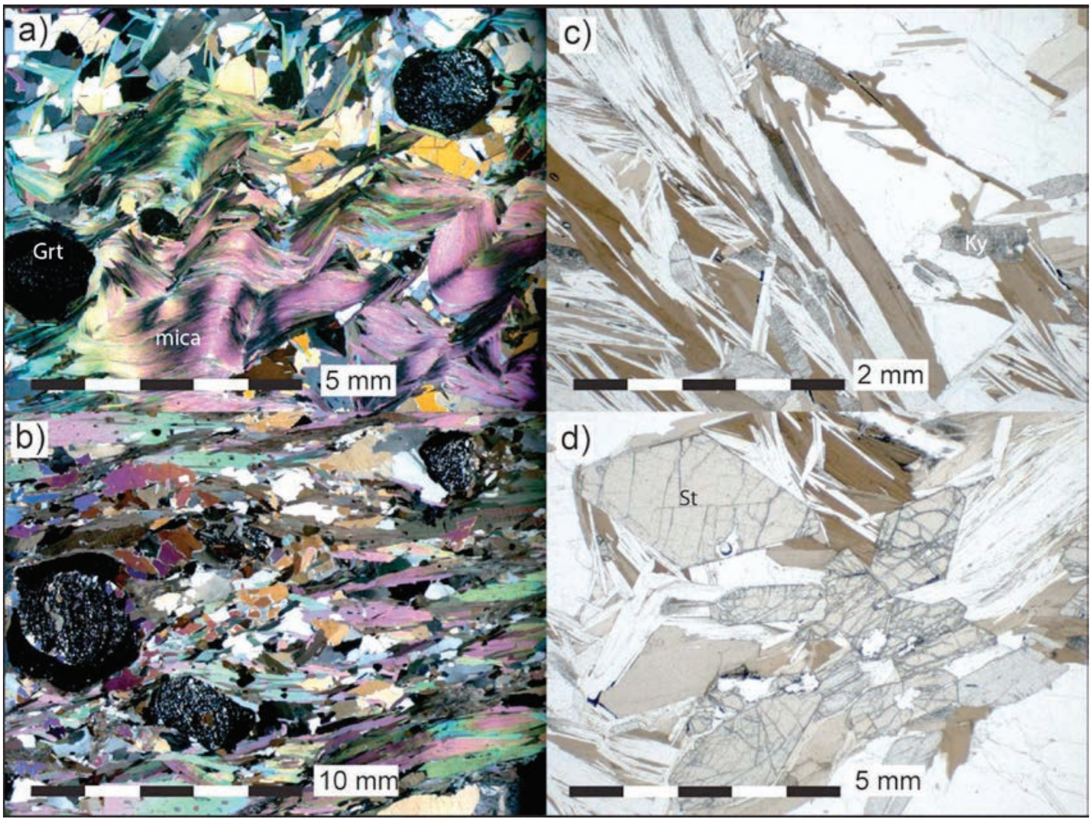

Figure 3.4
a) Crenulated garnet-mica schist at Singhik shown in cross polarised light (XPL). b) Large garnets (Grt) displaying very strong zoning with syn-kinematic inclusion trails within the garnet core, surrounded by an inclusion free rim at Singhik (XPL). c-d) kyanite (Ky) and euhedral staurolite (St) crystals within a garnet-staurolite-kyanite schist at Seven Sisters waterfall (stop 3.2) shown in plane polarised light (PPL).

Myang (N 27.52737˚, E 88.60660˚)

The Myang fibrolite schist is important as it has a GHS geochemical signature (Mottram et al., 2014), and therefore represents the 'geochemical' break associated with the MCT. Myang marks the southern-most boundary of a package of rocks within the MCT-zone that has a GHS geochemical signature and consists of fibrolit ic sillimanite-muscovite schist, calc-silicate, amphibolite and quartzite.

Figure 3.5
Hand specimen photograph of the large euhedral garnets in the fine grained mica schist at Rang Rang.

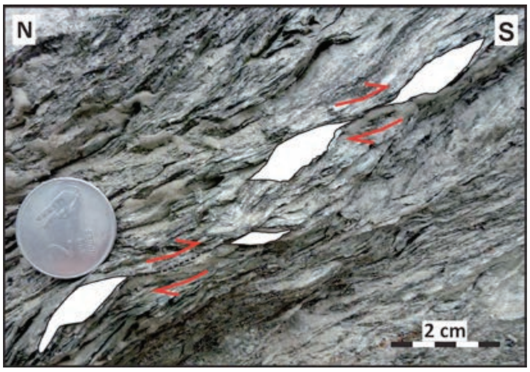

Figure 3.6
Shear bands are clearly developed in the micaceous schist at Rang Rang showing a top-to-south sense of shear (adapted from Mottram et al., 2014).

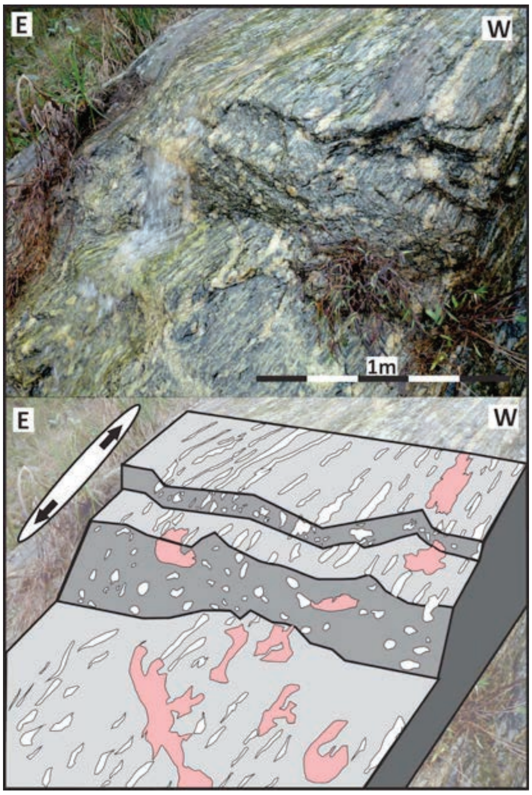

Figure 3.7
Photograph and sketch of the deformed L-tectonite Lingtse gneiss at Manul (adapted from Mottram et al., 2014).

Toong (N 27.55082˚, E 88.64648˚)

Between Toong and Chungthang the road cuts through a series of high cliffs of calc-silicate, with a spectacular gorge below. The prominent cliffs (Fig. 3.8) are markedly different from anything else seen in the MCT transect. The folded calc-silicate and quartzite which form this section are more resistant to deformation and erosion than the schist that is predominant at structurally lower levels. These rocks have also experienced higher metamorphic conditions demonstrated by sillimanite in the subordinate schist seen in this locality.

Chungthang (N 27.60157˚, E 88.64568˚)

Chungthang marks the northern-most limit of the 'MCT zone' in Sikkim. It sits at the confluence of the two rivers that flow from the western Lachen valley and eastern Lachung valley to the north.

The rocks at Chungthang are a complicated mix of quartzite, gneiss, pegmatite and melt veins (Fig. 3.9). The presence of brittle cross-cutting leucosome veins indicates the close proximity to the GHS where related melt most likely originated. The quartzite in this area yields a Paleoproterozoic to Archean detrital zircon signature, indicative of an LHS provenance. It is likely that at the upper levels if the MCT zone, close to the original protolith boundary, rocks of LHS and GHS provenance became interleaved during ductile shearing (Mottram et al., 2014). This may also explain why the rocks to the north of Myang are markedly different from the sections elsewhere in the MCT zone.

4 THE GREATER HIMALAYAN SEQUENCE

The Greater Himalayan Sequence (GHS) is a ~5-20 km thick package of high-grade metamorphic rocks which span the length of the Himalaya (Le Fort, 1975; Pecher, 1989). The GHS package has experienced granulite- facies metamorphism, partial melting, migmatisation, anatexis, leucogranite formation and a prolonged history of high-temperature ductile deformation. It is thought that the GHS rocks were buried to depths of over 20-30 km in the crust before being extruded due to movement on the MCT and STDS (Grujic et al.

Figure 3.8
Prominent cliffs of folded calc-silicate to the north of Toong along the road to Chungthang.

Figure 3.9
Leucogranite melt veins cross cut gneiss at Chungthang.

1996).

The GHS in the Sikkim Himalaya consists of a series of predominantly metapelitic rocks with subordinate quartzites, calc-silicates, orthogneisses, leucogranites and mafic rocks. The metapelites have experienced peak pressure and temperature conditions of ~800°C and 10 kbar (Ganguly et al. 2000), with partial melting occurring during the extended metamorphic history (Chakraborty et al. 2003; Harris et al., 2004, Rubatto et al., 2013). Monazite and zircon geochronology reveals that the GHS has a prolonged history of accessory phase growth during partial melting and amphibolite- granulite facies metamorphism during the Oligocene-Miocene (Rubatto et al. 2013). The geochronological (Catlos et al., 2004; Rubatto et al., 2013) and metamorphic data (Ganguly et al. 2000) indicate that the GHS in Sikkim consist of at least two units separated by a cryptic shear zone (Kellett et al., 2013; Figure 1.1). Potentially similar tectonic discontinuities have been identified within the GHS in Bhutan (Warren et al., 2011, Grujic et al., 2011) and Nepal (e.g., Groppo et al., 2009, Carosi et al., 2010; Montomoli et al., 2013; Larson et al., 2013) and are thought to have formed during exhumation of the GHS.

Finally, the occurrence of strongly retrogressed mafic granulites in the highest structural levels of the GHS (Rolfo et al., 2008; own observations) suggest that this segment of the GHS has been exhumed from the base of the south Tibetan crust similar to the situation in western Bhutan (Grujic et al., 2011) and eastern Nepal (Cottle et al., 2009; Groppo et al., 2007). The GHS is well exposed in road cuts and trekking routes through several locations throughout the Sikkim Himalaya; Yuksom in the west, Tsomgo lake road to Natu La in the east and the Lachen and Lachung valleys in the north. This section of the virtual fieldtrip continues from the MCT (section 3) at Chungthang up into the Lachung valley in the North of Sikkim (Figure 3 .1) where the GHS rocks can be seen.

Chungthang (N 27.60157˚, E 88.64568˚)

Chungthang, as described in section 3.7, marks the start of the GHS proper, where the upper amphibolite- to granulite- facies gneisses are cross cut by leucogranite veins. The transition from LHS to GHS through the zone of deformation associated with the MCT, as described in the previous section, does not mark a sharp break in either lithology or metamorphic grade. There is a gradual increase in peak metamorphic temperature from ~500°C to ~800°C with a relatively small variation in pressure conditions from ~8-10 kbar through the LHS to GHS transition (Dubey et al. 2005; Dasgupta et al. 2009; Mottram, 2014). The rocks of the GHS crop out in both the Lachen and Lachung valleys of North Sikkim. The Mw 6.9 Sikkim earthquake of September, 2011 caused some large landslides in this region (Rajendran et al., 2011; Mahajan et al., 2012; Fig. 4.1) exposing

Figure 4.1
Large landslides disrupted the rocks in the North of Sikkim after the September 2011 earthquake. This photograph shows the fresh outcrops of gneiss exposed in the Lachung valley.

Figure 4.2
Discontinuous mafic sills and boudins intruded into the metapelitic gneiss of the lower Lachung valley.

some very fresh, if rather unstable, exposure of the rocks in this area.

Bhimnala falls (N 27.63433˚, E 88.70430˚)

The rocks exposed along the road between Chungthang and the Bhimnala Falls show some key features of the geology of the GHS in the Sikkim Himalaya. Mafic sills and boudins can be seen in the GHS throughout the Sikkim Himalaya (Faak et al., 2012) and beyond (Figs. 4.2, 4.3). The lack of geochronological constraints on when the mafic bodies were intruded makes it difficult to interpret their geological significance, however they could be related to the felsic orthogneiss bodies present in the GHS or represent bodies intruded early in the history of the Himalayan collision. Previously determined ages range from Neoproterozoic (Cottle et al., 2009) to Miocene (Grujic et al., 2011). Throughout the eastern Himalaya, similar mafic boudins locally preserve evidence for high-pressure metamorphism (e.g. Lombardo and Rolfo, 2000; Cottle et al., 2009, Groppo et al., 2007; Grujic et al., 2011), including an example in northern Sikkim (Rolfo et al., 2008).

The rocks at Bhimnala falls are migmatitic metapelitic gneiss with an assemblage containing garnet+biotite+quartz+plagioclase+K-feldspar+sillimanite+spinel. The rocks are pervasively ductily deformed (Fig. 4.4), with the migmatitic banding folded into recumbent folds. These rocks have undergone peak metamorphic conditions of ~800°C and 9 kbar, where they equilibrated above the solidus. Evidence of spinel breakdown textures at the edge of garnets suggests that the rocks decompressed into the spinel (+cordierite) field on the retrograde path during isothermal decompression (Mottram, 2014). Monazite data from these rocks indicates that they had a prolonged history of accessory phase growth, starting in the late Oligocene and continuing until the mid-Miocene (Catlos et al., 2004; Rubatto et al. 2013; Mottram, 2014). The protracted history of monazite growth suggests the GHS rocks were at depth within the thickened crust for several tens of million years.

Lachung (N 27.68598˚, E 88.73853˚)

The rocks exposed between Bhimnala falls and the village of Lachung represent further exposures of pelitic gneiss, migmatite (Fig. 4.5), mafic bodies, calc-silicate (Fig. 4.6) and leucogranite. Leucogranite bodies are present throughout the GHS of the Himalaya and formed due to the melting of

Figure 4.3
Mafic boudins within a metapelitic gneiss in the Lachung valley.

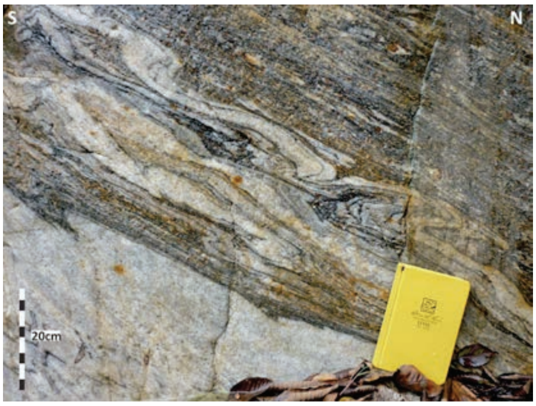

Figure 4.4
Ductily folded migmatitic metapelite outcropping at Bhimnala falls. Garnets with pressure shadows can be seen in the top right of the photograph.

Figure 4.5
Folded melt vein with well-developed biotite selvage in a GHS migmatite within the Lachung valley.

metapelitic GHS source rocks (Guillot and Lefort, 1995). Leucogranite at the top of the GHS package are described in section 5 and in Kellett et al. (2013).

Within the village of Lachung is an example of a GHS orthogneiss similar in appearance to the Lingtse gneiss which intrudes the LHS rocks in Sikkim (i.e. those at location 3.1 Tashi viewpoint). These orthogneisses represent pre-Himalayan granites which were intruded into the GHS protolith. The body at Lachung has been dated at ca. 520-490 Ma (Mottram et al., 2014) indicating it may have been intruded during a widespread Cambro-Ordovician orogeny (Gehrels et al. 2006).

North to Yumesamdung (N 27.93057˚, E 88.73407˚)

The road continues north through GHS rocks from Lachung to Yumesamdung in the extreme north of the area (close to Gurudongmar Lake-section 5.5). The metapelitic gneiss exposed along the way continues to display the features outlined in the localities above, with prominent sillimanite-grade metamorphism (Fig. 4.7.). Due to an apparent tectonic discontinuity between the upper and lower structural levels of the GHS as revealed by distinctly younger monazite ages in the structurally higher samples (Rubatto et al., 2013), it has been suggested that there may be at least one discrete thrust preserved within in the pervasively deformed GHS of the Sikkim Himalaya. This structure may be similar in nature to cryptic thrusts found in Bhutan (Warren et al. 2011; Grujic et al. 2011), eastern Nepal (Larson et al., 2013) and western Nepal (Groppo et al., 2009; Carosi et al. 2010) that facilitated exhumation of the GHS at different stages of the collision.

5 SOUTH TIBETAN DETACHMENT SYSTEM

For the final portion of the field trip we travel to northern Sikkim to examine a spectacularly exposed section of the South Tibetan detachment system (STDS) in northern Sikkim (Fig. 1.1). We will focus on the structurally uppermost GHS rocks, which are deformed by the detachment system north of the village of Thanggu, near the India-Tibet border. These rocks preserve a history of Tertiary metamorphism and partial melting, deformation, and exhumation in the footwall of a large scale, orogen-parallel detachment.

The STDS is a set of low-angle normal-sense structures that cuts through some of the highest peaks of the Himalayan orogen, including Dhaulagiri, Annapurna, and Everest (Chomolungma), to name a few, and separates high-grade metamorphic rocks of the GHS in its footwall from low grade metamorphic to sedimentary rocks of the Tethyan sedimentary sequence (TSS) in its hanging wall. The detachment system is situated along strike of the crest of the range, where the steep, deeply-incised southern front of the

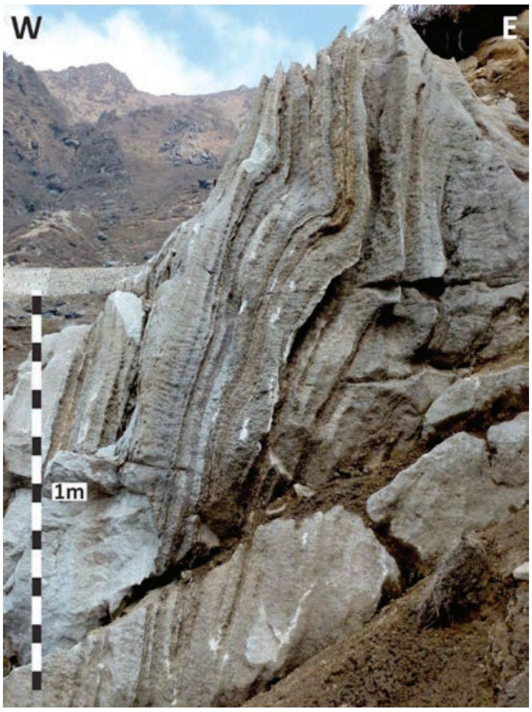

Figure 4.6
Folded calc-silicate with distinctive weathering pattern common in calc-silicate bodies.

Figure 4.7
Prominent sillimanite lath in a GHS sillimanite gneiss from Yumesamdung in the upper Lachung valley.

Himalayan mountain chain meets the broad, undulating high-altitude hills of the Tibetan plateau (Fig. 1.1).

The formation of normal-sense structures like the STDS which seem to indicate slip occurred at low angles (≤30°dip) is in apparent contradiction with Anderson's theory of basic fault mechanics, which predicts that normal-sense structures will form at relatively high (~60°) dip angles, while low-angle structures should be thrust sense (Anderson, 1951). Partly for this reason, geologists did not recognize low-angle normal sense detachments (LANDs, also sometimes referred to as LANFs - low-angle normal faults) in the field until the 1970's and 1980's (e.g., Armstrong, 1972; Davis and Coney, 1979; Wernicke and Burchfiel, 1982). LANDs are now known to be common structures, and have been mapped in several tectonic environments (e.g., extensional provinces such as the Basin and Range, metamorphic core complexes such as those in the Cordillera, slow-spreading mid-ocean ridges such as the Mid- Atlantic Ridge, and active collisional orogens such as the Himalaya). LANDs from these different tectonic settings share many common features, including: low (≤30°) dip angles; a contrast in structural style above and below the detachment; pooling of magma in the footwall at the detachment surface (often attributed to decompression melting of footwall rocks as they are denuded and resulting in a thermal and rheological contrast across the detachment); and, the juxtaposition of high-grade metamorphic rocks exhumed from the middle or lower crust in the footwall against unmetamorphosed or low-grade upper crustal rocks in the hanging wall. Some of the first studies on LANDs, in metamorphic core complexes of the Basin and Range extensional province of the southwest USA and the North American Cordillera, pointed to an exclusively extensional tectonic setting for their formation. The STDS was the first LAND discovered to have accommodated lithospheric contraction and remains the best studied worldwide, although to date, kinematically similar structures have been identified in other active and ancient orogens including: Pamir (e.g., Brunel et al., 1994); Canadian Cordillera (e.g., Carr et al., 1987; Brown and Gibson, 2006), and Hellenides (e.g., Xypolias and Kokkalas, 2006; Ring et al., 2007).

The STDS was first described by Burg et al. (1984) as a normal fault that deformed leucogranites at the top of the GHS metamorphic package, and that in places juxtaposed low-grade metamorphosed Jurassic schists against staurolite-kyanite gneiss. Investigating crystallographic preferred orientations in quartz crystals within leucogranites in southern Tibet east of Bhutan, Burg et al. (1984) demonstrated that the upper boundary of the GHS was a shear zone of gently-dipping mylonite gneiss hundreds of metres thick that had an opposite shear sense to the regional thrusting. They further demonstrated that shearing post-dated emplacement of the leucogranites, which at that time were already suspected to be produced from partial melting within the GHS above the MCT. This timing relationship demonstrated that the normal-sense structure was likely Miocene in age, and thus coeval to either the MCT or the MBT. Burg and colleagues noted the apparent incongruity of a north-directed normal-sense ductile shear zone within the south-directed thrust-sense Himalayan orogen, and explained its formation by sliding of the TSS along a gravity-driven décollement (Burg et al., 1984).

Burchfiel and Royden (1985), noting the along-strike continuity of the structure, further suggested that it may have accommodated as much as tens of kilometres of extensional northward displacement of the TSS, and probably formed after development of the TSS fold and thrust belt and coevally with leucogranite intrusion and thrusting on the MCT or MBT. It was later confirmed that the STDS and the MCT were indeed coevally active (Hodges et al., 1992), and that the STDS extends west as far as NW India (Herren, 1987; Kündig, 1988).

The STDS in Sikkim

In Sikkim, rocks deformed by the STDS are accessible along its northern border at intermediate altitudes (4000-5500 m above sea level) by road or trekking trails. The contrast in metamorphic grade and hence compentency of rocks in the hanging wall and footwall of the STDS is marked, and the arid Tibetan plateau is sparsely vegetated,

Figure 5.1
Digital elevation model of northern Sikkim showing the trace of the STDS, as well as main foliation of the upper GHS, modified from Kellett et al. (2013).

Table 5.1
Virtual field trip stops for South Tibetan detachment system.

	Locality	Lat	Long	Description
5.1	Dongkung section	28.01477	88.59277	transect across base of STDS
5.2	N of Dongkung section	28.02326	88.59514	Large-scale cross-sectional views of STDS, Tethyan Himalaya hanging wall and GHS footwall
5.3	Eastern ridge	28.01139	88.60420	Northernmost outcrop of STDS
5.4	Gurudongmar Lake	28.03472	88.70833	float and outcrop in the uppermost footwall of the STDS

such that the STDS trace can be observed relatively clearly from satellite imagery (Fig. 5.1). It can be seen in Fig. 5.1 that although the STDS is regionally an east-west striking and north-dipping structure, the detachment system locally dips towards NE in Sikkim, and is offset by a small, north-south striking extensional fault, apparently synthetic to major NS-striking structures that form late graben systems such as the Yadong graben (SE corner of Fig. 5.1) across the Himalayan chain and are seismically active (Pradhan et al., 2013).

The road which today travels through Thangu wraps around to the east once north of the Himalayan range, to provide access to Gurudongmar Lake, one of the highest lakes in the world (5148 m) and a sacred pilgrimage route for Buddhists, Sikhs and Hindus alike. The first stop for this section of the virtual field trip is near Dongkung, along this road north of Thangu (Fig. 1.1, Table 5.1) where GHS rocks are deformed in the footwall of the STDS. Note that an "inner line permit" is needed to access the areas to the north of Thangu.

Dongkung section (N 28.01477˚, E 88.59277˚)

The Dongkung transect is located north of Thangu, and west of the road leading to Gurudongmar Lake (Figs. 5.1, 5.2, Table 5.1). Dongkung itself comprises a group of pastoral structures north of the geological section. Outcrop is relatively continuous along a gully. The GHS at this site comprises variably migmatitic, locally mylonitic metapelitic (Fig. 5.3a, b) and augen (Fig. 5.4a) gneiss with local quartzite layers and mafic lenses (Fig. 5.4b). Leucosomes suggest in situ partial melting (e.g. Fig. 5.3a,b), while abundant cross-cutting leucogranite dykes (locally aplitic) (e.g. Fig. 5.4a) indicate transported melt, likely derived from structurally lower units in the GHS package.

The main fabric in the rocks dips to NE north of the southernmost outcrops (N 28.014777, E 88.592767, ~4730 m). The dominant shear sense transitions from top-up-to-south to top-down-to-northeast with pervasive top-northeast shear sense indicators observable from 28.016050, 88.592817 and continuing northward. Sillimanite and quartz define mineral stretching lineations that on average plunge shallowly towards NNE (Fig. 5.5a) while biotite and fine gneissic banding defines the main foliation in gneiss (Fig. 5.5a) and mylonite (Fig. 5.5b). Discrete brittle fault surfaces coated in chlorite slickenfibres exhibit minor displacement and are parallel to stretching lineations. Top-down-to-northeast shear sense indicators in outcrop include shear bands (Fig. 5.2a), -type K-feldspar porphyroclasts, including large -type structures formed around mafic lenses (Fig. 5.4d), bookshelf sliding in mafic lenses (Fig. 5.3b), and weak S-C fabric. Crystallographic preferred orientation fabrics in quartz-rich metapelitic gneiss record well-defined type II crossed girdle fabrics (Fig. 5.6). This implies that dynamic crystallization of quartz was occurring during deformation, consistent with quartz defining the mineral stretching lineation. Moreover, these type II fabrics may indicate constrictional strain (Bouchez, 1978; Schmid and Casey, 1986). With the exception of SK63, the fabrics are broadly symmetrical and cannot be used to determine shear sense. SK63, however, shows a strong asymmetry indicating a top-up-to-the-south sense shear. Such a shear sense is antithetic to the dominant observed direction, however, SK63 was collected from a localized region of asymmetric folding in which the dominant regional mylonitic fabric was not developed. The shear sense recorded by this sample may thus preserve the relict deformation fabric that predates the main STDS mylonite fabric regionally preserved in the area, indicating that top-north deformation overprints an earlier top-south deformation.

Leucogranite dykes show little internal deformation in outcrop, but in thin section some of them exhibit quartz grain size reduction and subgrain rotation recrystallization, deformation twins in plagioclase, myrmekite, tartan twins in K-feldspar, and a preferred orientation of biotite and muscovite, indicating they have experienced subsolidus ductile deformation at relatively high temperatures (Kellett et al., 2013).

Both outcrop and thin section observations indicate that STDS deformation occurred subsequently to peak temperature metamorphism under sillimanite-stable conditions. Shear bands wrap around garnet grains, leucosomes record subsolidus deformation and are cut by shear bands (e.g. Fig. 5.2 a,b), and fibrolite is typically associated with shear bands. These observations are corroborated by in situ Th-Pb monazite geochronology of gneisses (e.g. SK63 of Fig. 5.6). Monazite included in garnet are ≥23.4 Ma, while monazite associated with shear bands in the matrix are as young as 14.6 Ma (Kellett et al., 2013). Zircon rims from cross-cutting and weakly-de-

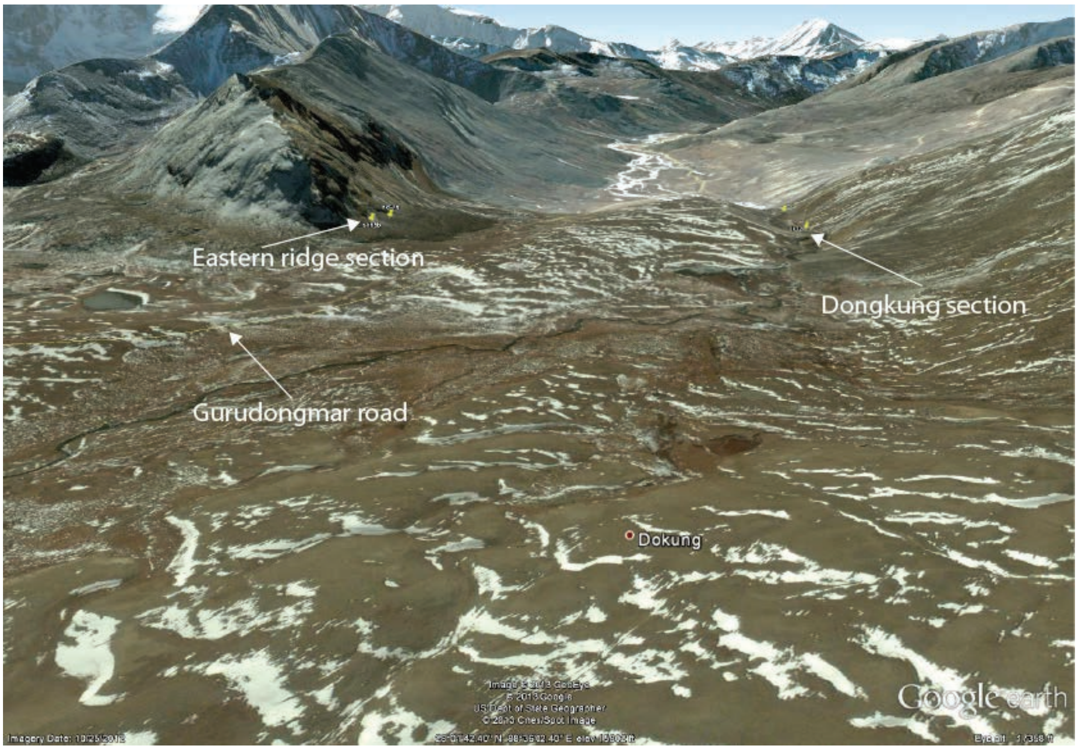

Figure 5.2
This view shows the locations of the Dongkung and Eastern ridge sections on either side of the road to Gurudongmar Lake, both of which record STDS deformation.

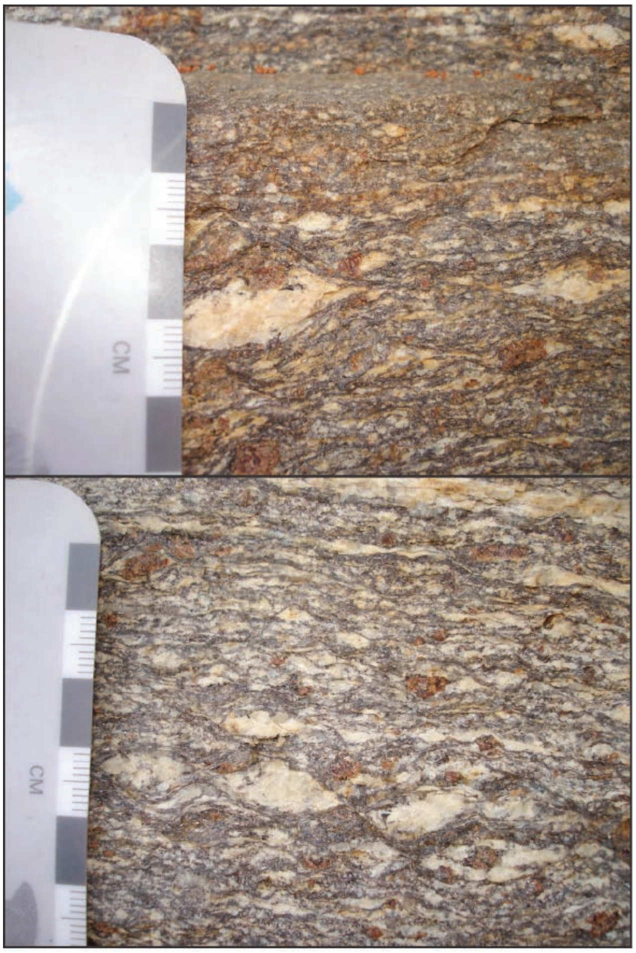

Figure 5.3
Shear bands cut leucosomes and indicate top-down-to-north (right) shear sense. View is towards west in both photographs.

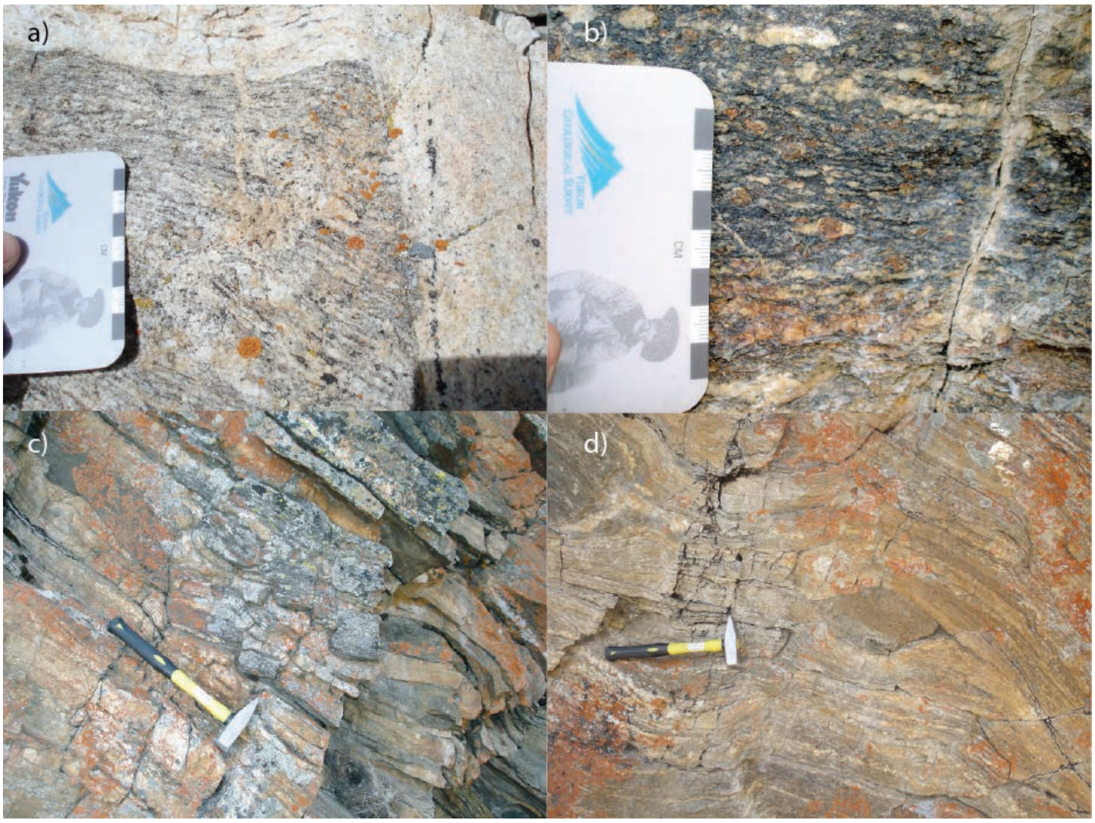

Figure 5.4
a) Migmatite augen gneiss with large concordant leucosome at top of photo, cut at a high angle by a relatively undeformed leucogranite dyke. b) Pressure shadows around garnet grains in mylonite gneiss. c) Bookshelf sliding of blocks in fractured mafic lens. Hammer handle is ~30 cm. d) Asymmetric mafic boudin hosted by migmatite gneiss. View is towards west in all photographs.

formed leucogranite dykes also indicate crystallization until ca. 14 Ma (U-Pb ages) at >700 °C (Ti-in-zircon). These data together suggest that the footwall of the STDS was deformed by top-down-to-the-north shear between 23.6-14 Ma. Near identical ages for last zircon growth, last monazite growth, retention of Ar in muscovite and retention of fission tracks and He in apatite illustrate the transient rapid cooling of this section of the STDS during Middle Miocene (Kellett et al., 2013).

N of Dongkung section (N 28.02326˚, E 88.59514˚)

Walking out of the gully to the north, one gains a spectacular cross-sectional view of the STDS towards the east (Fig. 5.7). To the NE, the undulating topography forming the southernmost extent of the Tibetan plateau is comprised of black slate of the TSS. Other TSS lithologies mapped in the hanging wall of the STDS in Sikkim include Devonian to Jurassic carbonate and clastic rocks (Wu et al., 1998; Edwards et al., 2002), with a sliver of Neoproterozoic-Cambrian slate, schist intercalated with sandstone, quartzite and marble mapped further to the west (Pan et al., 2004). To the SW, high-grade gneiss and leucogranite of the GHS exhibit a more resistant, blocky weathering profile, and form the northernmost peaks of the Himalayan range. The two - part nature of the STDS can be observed in Figure 5.7. The footwall GHS rocks comprise a diffuse, ≤ 1km thick ductile shear zone with top-to-NE sense of shear. This ductile shear zone is cut by a steeper, ductile-brittle fault that juxtaposes the unmetamorphosed TSS hanging wall against the amphibolite- to granulite-grade gneisses. These structures may be akin to the better known Lhotse (lower) and Qomolangma (upper) detachments which cut through Mt. Everest (e.g. Searle et al., 2003). The lower structure has been interpreted as the upper boundary to a mid-crustal channel of deformed rock that flowed to the south during Miocene, while the upper boundary

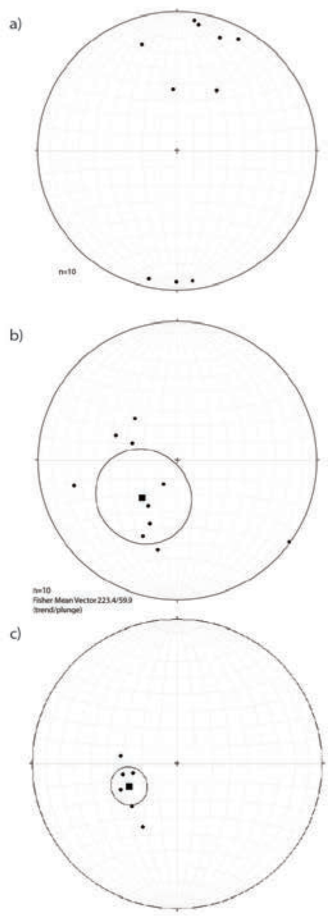

Figure 5.5
a) Stretching lineations at Dongkung section predominantly dip shallowly towards NNE. b) Poles to foliation planes indicate that main foliation dips moderately towards NE, while mylonitic fabric c) dips somewhat more shallowly towards ENE. Stereonets plotted using Stereonet v.7.2.1 by R. Allmendinger.

is interpreted to be a later Miocene normal fault that has unroofed and cooled the paleo-channel (Kellett and Grujic, 2012, Kellett et al., 2013).

Eastern ridge (N 28.01139˚, E 88.60420˚)

Following the road towards Gurudongmar Lake north from the Dongkung section, one can access a ridge to the east of the valley. Here called the eastern ridge (Fig. 5.2), outcrop comprises migmatized, garnet-biotite-sillimanite gneiss and augen gneiss of the GHS (Fig. 5.8b, c), locally restitic in composition, and local bands of both biotite-bearing dark quartzite (Fig. 5.8a) and calcsilicate. As in the Dongkung section, STDS deformation appears to have postdated peak metamorphism and occurred under sillimanite-stable conditions. Muscovite is locally associated with

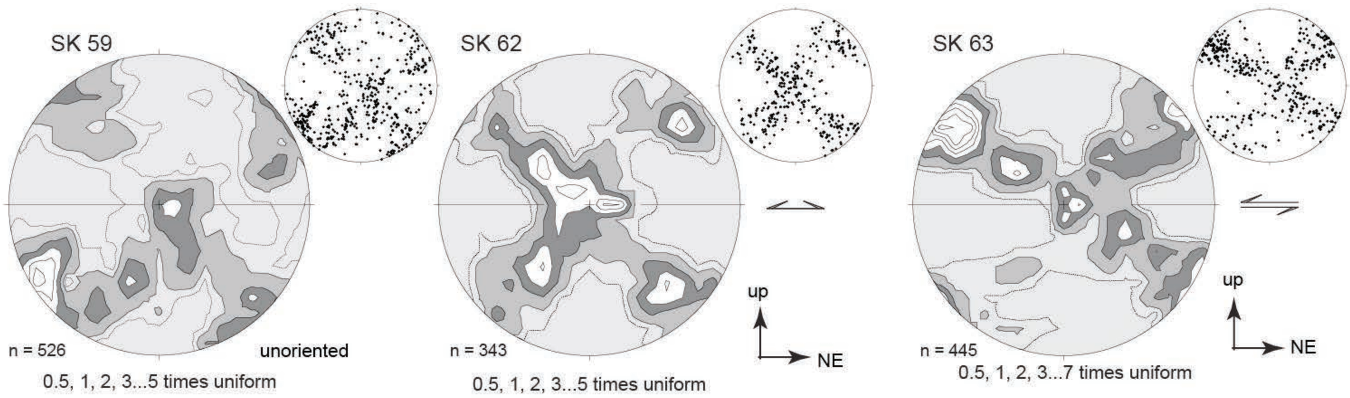

Figure 5.6
Crystallographic preferred orientations of quartz in quartz-rich GHS metapelitic gneiss from the Dongkung section illustrating the non-coaxiality of deformation. SK 62 is a garnet-biotite-sillimanite (in order of increasing abundance) gneiss with fibrolite occurring in shear bands, myrmekite, dominantly grain boundary migration recrystallization with local subgrain rotation recrystallization in quartz, biotite+quartz+sillimanite strain shadows around pervasively fractured garnets. Internal fabric in garnets is at a high angle to the gneissic fabric. Accessory monazite in this sample yielded Th-Pb ages ranging ~32-14.6 Ma with youngest monazite included in garnet yielding 23.6 Ma (Kellett et al., 2013). SK 63 is a garnet-biotite- sillimanite gneiss with dominant grain boundary migration recrystallization and minor subgrain rotation recrystallization of quartz, deformation twins in plagioclase, and myrmekite. Sillimanite occurs both as prismatic grains and as fibrolite and, along with biotite and quartz ribbons, defines the main fabric of the rock. Garnets lack internal fabric and are pervasively fractured. SK 59 is a sillimanite-garnet-biotite gneiss with myrmekite texture, deformation twins in plagioclase, undulose extinction in quartz, and biotite+quartz pressure shadows around garnet.

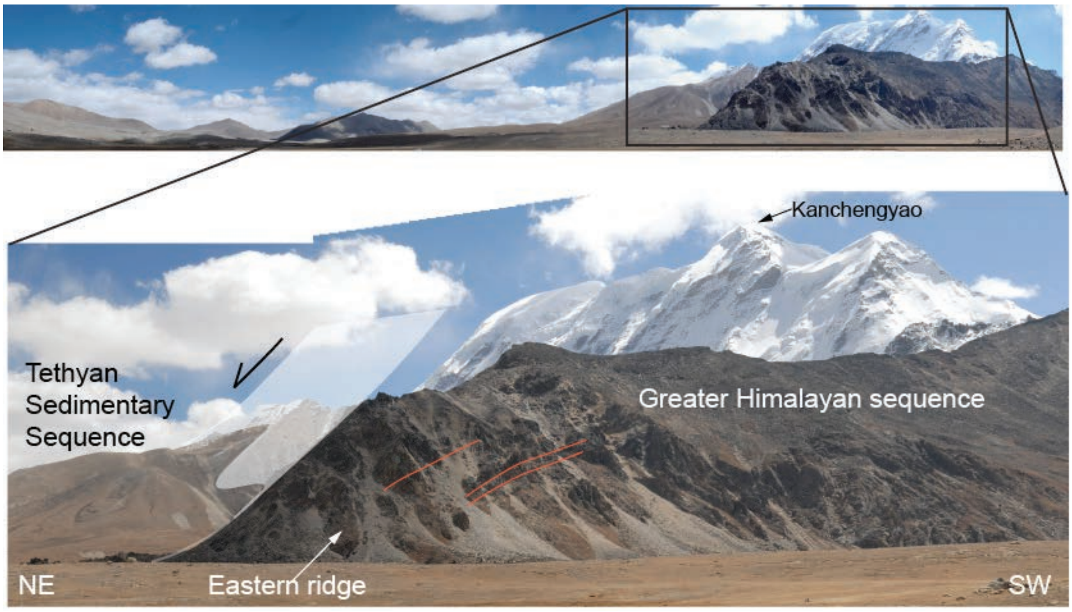

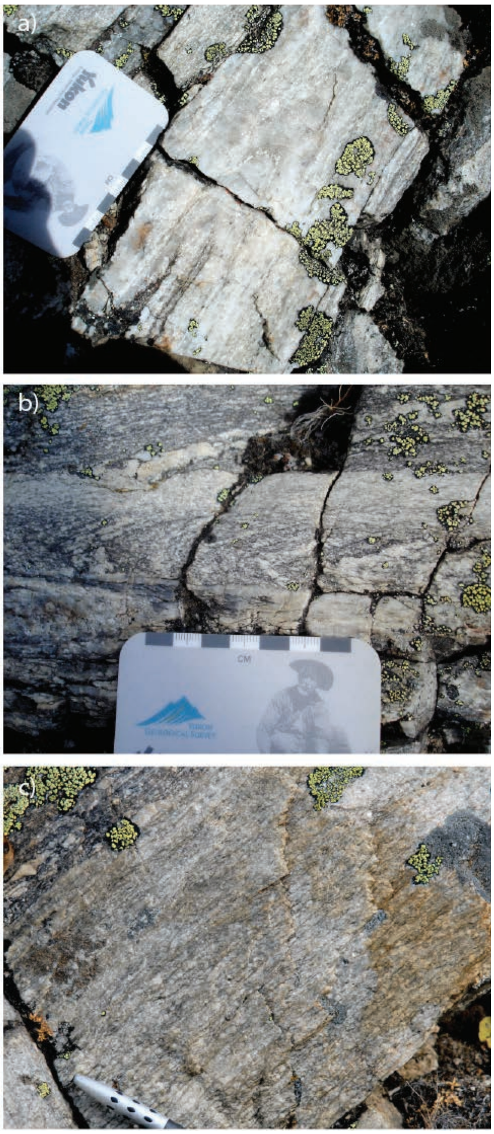

Figure 5.7
The outcrops identified by stars in the lower photo are 75 m apart. The dip surface of the upper discrete fault is show in white, while red lines show the shallower dip of the lower diffuse ductile shear zone in its footwall. The stark contrast in lithology and weathering profile was used to delineate the regional trace of the STDS in Sikkim shown in Figure 5.1. Lower photograph is modified from Kellett et al. (2013).

Figure 5.8
a) Isoclinal fold in quartzite. b) Isoclinal fold cut by mylonite fabric developed in augen gneiss and leucosomes. c) S-C fabric in augen gneiss. View in all photographs is towards E.

shear bands. Like the Dongkung section, gneisses are locally mylonitized and folded, however mylonitiza tion is more generally pervasive. Rocks exhibit isoclinal folds that predate mylonitization (Fig. 5.8a,b) and well-developed S-C fabric (Fig. 5.8c) with kinematics consistent with the Dongkung section, top-down-to-NE. Fibrolite is pervasive and particular ly defines the mylonitic foliation. In thin section, flame perthite is preserved, and dynamic recrystallization of quartz by grain boundary migration is pervasive. Crystallographic preferred orientations of quartz c-axes in quartz-rich samples from this area record that dynamic recrystallization as strongly developed, largely symmetric, point maxima (Fig. 5.9) This pattern indicates activation of the prism <a> plane (Schmid and Casey, 1986) and is significantly dif-

Figure 5.9
Crystallographic preferred orientations in quartz from a) feldspar-bearing quartzite and b) mylonitized augen gneiss.

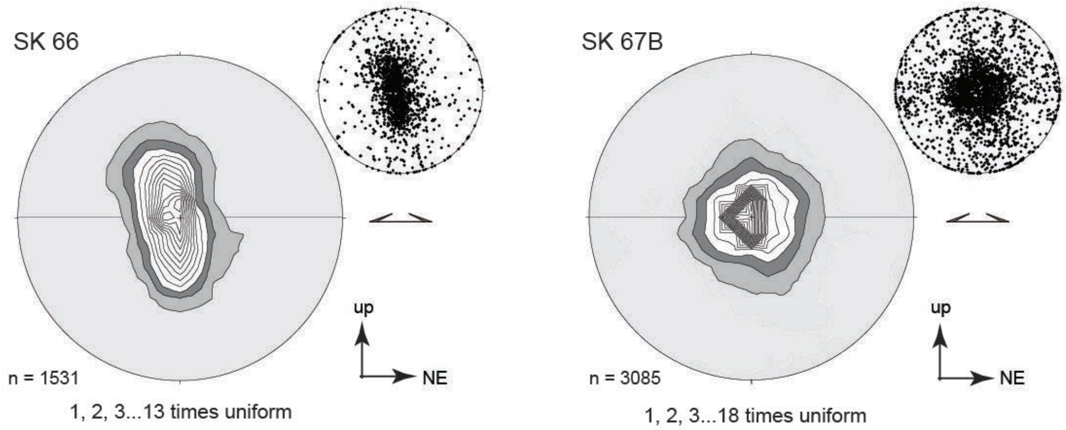

Figure 5.10
View is tilted and towards south. North-south length of Gurudongmar Lake is 1.8 km. The interpreted trace of the South Tibetan detachment system upper structure is shown in red, separating GHS rocks in the footwall to the south from TSS rocks in the hanging wall to the north.

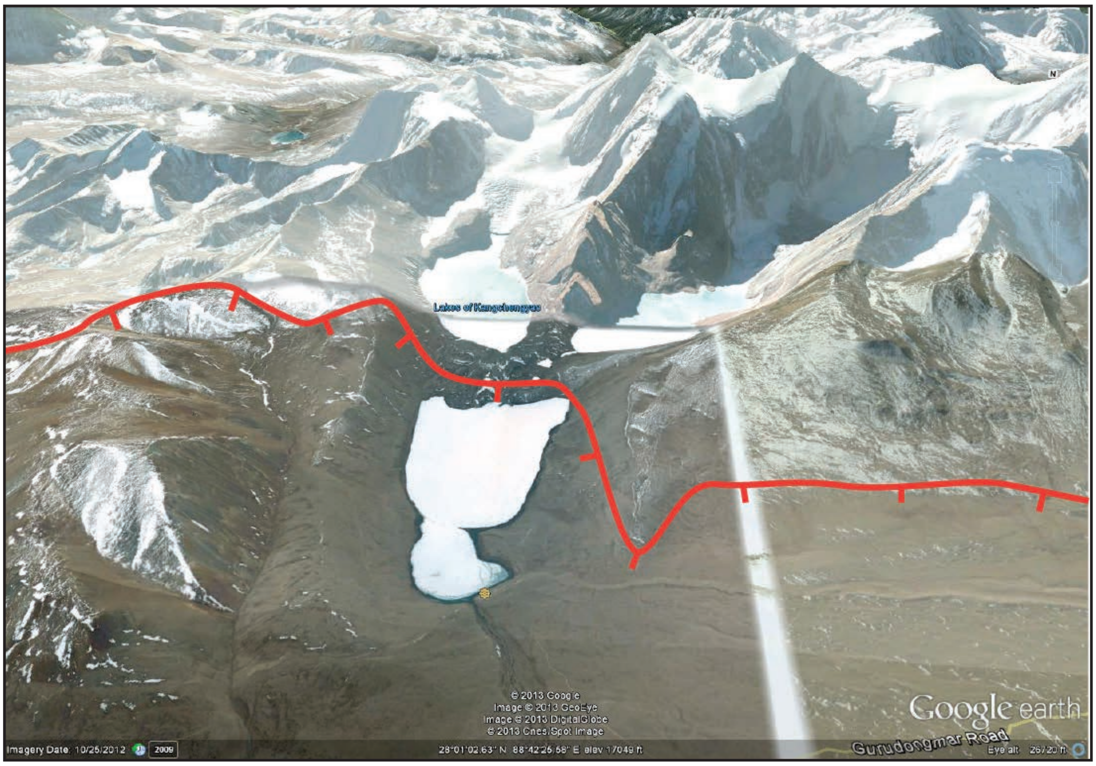

Figure 5.11
View to SSW of footwall GHS rocks that form Gurudongmar and neighbouring peaks, lining the south shore of Gurudongmar Lake. The path that circles the lake can be viewed along the shoreline. A thick layer of glacial moraine till separates the lake from the mountains.

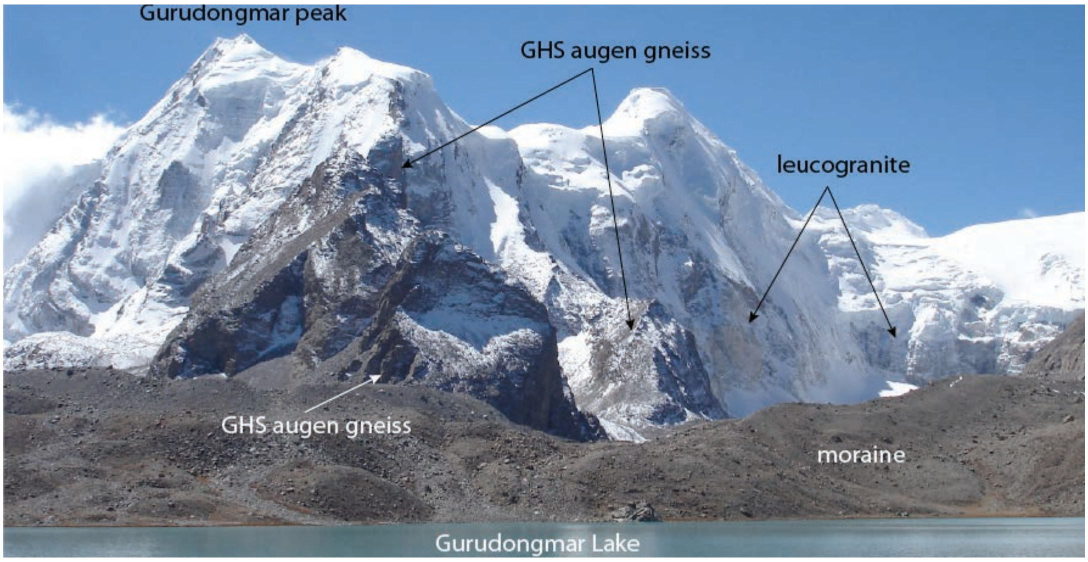

Figure 5.12
Leucogranite bodies stand out with their pale weathered surface in comparison to the darker augen gneiss. Lake surface elevation is 5154 m, and Gurudongmar peak reaches ~6500 m above sea level.

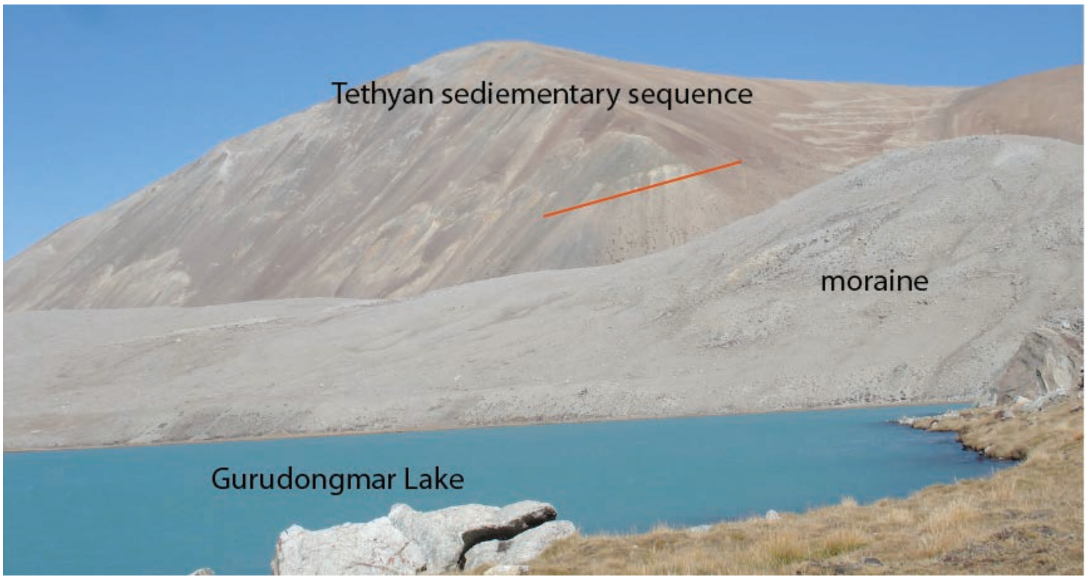

Figure 5.13
The hill in the background is comprised of north-dipping grey, tan and rusty layers (N-dipping tan layer highlighted with a white line intentionally below outcrop) of relatively incompetent rock, likely slate and other siliciclastic sedimentary rocks of the TSS. Comparing with Figures 5.10 and 5.12, the STDS passes just beneath the lake, with its surface expression buried by glacial till.

ferent than the type II fabrics recorded structurally lower in the Dongkung section (Fig. 5.6). The change in c-axis orientations may indicate that the present fabrics developed in a kinematic environment approximating plane strain deformation. Moreover, the dominance of prism <a> slip is consistent with these structurally higher fabrics being developed at high temperatures during non-coaxial strain (e.g. Lister and Dornsiepen, 1982; Law et al., 1990).

Comparatively, rocks at this site record a higher degree of crystal-plastic deformation than in the Dongkung section. This is evidenced by the more pervasive mylonitization, developed S-C fabric, crystallographic preferred orientation patterns in quartz and the generally finer grain size.

This strain localization could be rheologically controlled by the relatively more quartz-rich lithologies at eastern ridge, or by locally higher strain rates up-structural-section, consequently preserving a strain gradient.

Gurudongmar Lake (N 28.03472˚, E 88.70833˚)

Gurudongmar Lake is the final stop in this northern section. The lake sits on the southernmost edge of the Tibetan plateau and reflects the north face of Gurudongmar peak and neighbours in its waters (Figs. 5.10, 5.11). These peaks south of the lake comprise gneiss as well as substantial leucogranite bodies (Fig. 5.12). On the eastern flank of the lake, gently north-dipping, variably incompetent and bedded outcrop is diagnostic of TSS rocks (Fig. 5.13), also evidenced by abundant slate float occurring along the path which circumnavigates the lake.

REFERENCES

Ahmad, T., Harris, N., Bickle, M., Chapman, H., Bunbury, J. and Prince, C. 2000. Isotopic constraints on the structural relationships between the Lesser Himalayan Series and the High Himalayan Crystalline Series, Garhwal Himalaya. Geological Society of America Bulletin, 112, 467-477.

Anderson, E. M., 1951. The dynamics of faulting. Edinburgh and London, Oliver and Boyd, 206 p.

Armstrong, R., 1972. Low-angle (denudation) faults, hinterla nd of the Sevier orogenic belt, eastern Nevada and western Utah. Geological Society of America Bulletin, 83, 1729.

Baranowski, J., Armbruster, J., Seeber, L., and Molnar, P., 1984. Focal depths and fault plane solutions of earthquakes and active tectonics of the Himalaya. Journal Geophysical Research, 89, 6918–6928.

Beaumont, C., Jamieson, R. A., Nguyen, M. H. and Lee, B., 2001. Himalayan tectonics explained by extrusion of a low-viscosity crustal channel coupled to focused surface denudation. Nature, 414, 738-742.

Bendick, R. and Bilham, R., 2001. How perfect is the Himalayan arc? Geology, 29, 791-794. Bhattacharyya, K. and Mitra, G., 2009. A new kinematic evolutionary model for the growth of a duplex - an example from the Rangit duplex, Sikkim Himalaya, India. Gondwana Research, 16, 697-715.

Bhattacharyya, K. and Mitra, G., 2011. Strain softening along the MCT zone from the Sikkim Himalaya: Relative roles of Quartz and Micas. Journal of Structural Geology, 33, 1105-1121.

Bilham, R., Gaur, V. K. and Molnar, P., 2001. Himalayan Seismic Hazard. Science, 293,1442-1444.

Bookhagen, B., and Burbank, D.W., 2010. Toward a complete Himalayan hydrological budget: Spatiotemporal distribution of snowmelt and rainfall and their impact on river discharge. Journal of Geophysical Research, 115, F03019.

Bouchez, J.L., 1978. Preferred orientations of quartz <a> axes in some tectonites: kinematic inferences. Tectonophysics, 39, 25-50.

Boyer, S.E. and Elliott, D., 1982. Thrust systems. American Association of Petroleum Geologists, 66, 1196-1230.

Brown, R.L. and Gibson, H.D., 2006. An argument for channel flow in the southern Canadian Cordillera and comparison with Himalayan tectonics: in Channel Flow, Ductile Extrusion, and Exhumation in Continental Collision Zones, Law, R., Searle, M.P., and Godin, L., ed., Geological Society, London, Special Publications, 268, 543-560.

Brunel, M., Arnaud, N., Tapponnier, P., Pan, Y., and Wang, Y., 1994. Kongur Shan normal fault: Type example of mountain building assisted by extension (Karakoram fault,eastern Pamir). Geology, 22, 707-710.

Burchfiel, B.C. and Royden, L.H., 1985. North-south extension within the convergent Himalayan region. Geology, 13, 679-682.

Burg, J.P., Brunel, M., Gapais, D., Chen, G.M., and Liu, G.H., 1984. Deformation of leucogranites of the crystalline Main Central Sheet in southern Tibet (China). Journal of Structural Geology, 6, 535-542.

Carosi, R., C. Montomoli, C., Rubatto, D and Visoná, D., 2010. Late Oligocene high temperature shear zones in the core of the Higher Himalayan Crystallines (Lower Dolpo, western Nepal). Tectonics, 29, (doi:10.1029/2008TC002400).

Carr, S.D., Parrish, R.R., and Brown, R.L., 1987. Eocene structural development of the Valhalla complex, southeastern British Columbia. Tectonics, 6, 175-196.

Catlos, E.J., Dubey, C.S., Harrison, T.M. and Edwards, M.A., 2004. Late Miocene movement within the Himalayan Main Central Thrust shear zone, Sikkim, north-east India. Journal of Metamorphic Geology, 22, 207-226.

Chakraborty, S., Dasgupta, S. and Neogi, S., 2003. Generation of migmatites and the nature of partial melting in a continental collision zone setting: an example from the Sikkim Himalaya. Indian Journal of Geology, 75, 38-53.

Cottle, J.M., Jessup, M.J., Newell, D.L., Horstwood, M.S.A, Noble, S.R., Parrish, R.R., Waters, D.J., and Searle, M.P., 2009. Geochronology of granulitized eclogite from the Ama Drime Massif: Implications for the tectonic evolutio n of the South Tibetan Himalaya. Tectonics, 28, TC1002, (doi:10.1029/2008TC002256).

Dasgupta, S., Chakraborty, S., and Neogi, S., 2009.

Petrology of an inverted Barrovian Sequence of metapelites in Sikkim Himalaya, India: Constraints on the tectonics of inversion. American Journal of Science, 309, 43-84.

Davis, G.H., and Coney, P.J., 1979. Geologic development of the Cordilleran metamorphic core complexes. Geology, 7, 120-124.

De, R., and Kayal., J.R., 2004. Seismic activity at the MCT in the Sikkim Himalaya, Tectonophysics, 386, 243-248.

DeCelles, P.G., Gehrels, G.E., Quade, J., and Ojha, T.P., 1998. Eocene – early Miocene foreland basin development and the history of Himalayan thrusting, western and central Nepal. Tectonics, 17, 741-765.

DeCelles, P.G. and Mitra, G., 1995. History of the Sevier orogenic wedge in terms of critical taper models, north east Utah and south west Wyoming. Geological Society of America Bulletin, 107, 454–462.

de la Torre, T.L., Monsalve, G. Sheehan, A.F., Sapkota, S., and Wu, F., 2007. Earthquake processes of the Himalayan collision zone in eastern Nepal and the southern Tibetan Plateau. Geophysical Journal International, 171, 718–738.

Drukpa, D., Velasco, A.A., and Doser, D.I., 2006. Seismicity in the Kingdom of Bhutan (1937-2003): Evidence for crustal transcurrent deformation. Journal of Geophysical Research, 111, B06301, (doi:10.1029/2004JB003087).

Dubey, A.K., Mishra, R. and Bhakuni, S.S., 2001. Erratic shortening from balanced cross sections of the western Himalayan foreland basin causes and implications for basin evolution. Journal of Asian Earth Sciences, 19, 765–777.

Dubey, C.S., Catlos, E.J., and Sharma, B.K. 2005. Modelling of P-T-t paths constrained by mineral chemistry and monazite dating of metapelites in relationship to MCT activity in Sikkim Eastern Himalayas. in: Metamorphism and Crustal Evolution, Thomas, H. (ed.). New Delhi, Atlantic Publishers, 250-282.

Edwards, M.A., Catlos, E.J., Harrison, T.M., and Dubey, C.S., 2002. We seek him now, we sought him then: 70 years of constraints on the STDS in Sikkim. 17th Himalaya- Karakoram-Tibet Workshop, Sikkim, India. Journal of Asian Earth Sciences, 20(Suppl. 1), 11-12.

Ekstrom, G.A., 1987. Broad band method of earthquake analysis, Ph. D. thesis, Harvard Univ., Cambridge, Mass.

Faak, K., Chakraborty, S., and Dasgupta, S., 2012. Petrology and tectonic significance of metabasite slivers in the Lesser and Higher Himalayan domains of Sikkim, India. Journal of Metamorphic Geology, 30, 599-622.

Ganguly, J., Dasgupta, S., Cheng, W., and Neogi, S., 2000. Exhumation history of a section of the Sikkim Himalayas, India: records in the metamorphic mineral equilibria and compositional zoning of garnet. Earth and Planetary Science Letters, 183, 471-486.

Gansser, A., 1964. Geology of the Himalayas. London/New York/Sydney: Wiley Interscience. 289 p.

Gansser, A., 1983. Geology of the Bhutan Himalaya, Birkhauser Verlag Basel, 181 p. Gehrels, G., DeCelles, P., Ojha, T.P., and Upreti, B.N., 2006. Geologic and U-Th-Pb geochronologic evidence for early Paleozoic tectonism in the Kathmandu thrust sheet, central Nepal Himalaya. Geological Society of America Bulletin, 118, 185-198.

Gehrels, G., Kapp, P., DeCelles, P., Pullen, A., Blakey, R., Weislogel, A., Ding, L., Guynn, J., Martin, A., McQuarrie, N., and Yin A., 2011. Detrital zircon geochronology of pre-Tertiary strata in the Tibetan-Himalayan orogen. Tectonics, 30, (doi:10.1029/2011TC002868).

Goswami, S. 2005. Inverted metamorphism in the Sikkim-Darjiling Himalaya: Structural, metamorphic and numerical studies. Doctor of Philosophy, University of Cambridge.

Goswami, S., Bhowmik, S.K. and Dasgupta, S. 2009. Petrology of a non-classical Barrovian inverted metamorphic sequence from the western Arunachal Himalaya, India. Journal of Asian Earth Sciences, 36, 390-406.

Groppo, C., Lombardo, B., Rolfo, F., and Pertusati, P., 2007. Clockwise exhumation path of granulitized eclogites from the Ama Drime range (eastern Himalayas). Journal of Metamorphic Geology, 25, 51-75.

Groppo, C., Rolfo, F., and Lombardo, B., 2009. P-T evolution across the Main Central thrust zone (eastern Nepal): hidden discontinuities revealed by petrology. Journal of Petrology, 50, 1149-1180.

Grujic, D., Casey, M., Davidson, C., Hollister, L.S., Kündig, R., 1996. Ductile extrusion of the Higher Himalayan Crystalline in Bhutan: Evidence from quartz microfabrics. Tectonophysics, 260, 21-43.

Grujic, D., Warren, C.J., and Wooden, J.L., 2011, Rapid synconvergent exhumation of Miocene-aged lower orogenic crust in the eastern Himalaya. Lithosphere, 3, 346-366, (doi:10.1130/L154.1).

Guillot, S. and Le Fort, P., 1995. Geochemical constraints on the bimodal origin of High Himalayan leucogranites. Lithos, 35, 221-234.

Gupta, S., Das, A., Goswami, S., Modak, A., and Mondal, S. 2010. Evidence for structural discordance in the inverted metamorphic sequence of Sikkim Himalaya: Towards resolving the Main Central thrust controversy. Journal of the Geological Society of India, 75, 313-322.

Harris, N., Caddick, M., Kosler, J., Goswami, S., Vance, D., and Tindle, A., 2004. The pressure-temperature-time path of migmatites from the Sikkim Himalaya. Journal of Metamorphic Geology, 22, 249-264.

Hazarika, P., Kumar, M.R., Srijayanthi, G., Raju, P.S., Rao, N.P. and Srinagesh, D.,2010. Transverse tectonics in the Sikkim Himalaya: evidence from seismicity and focal- mechanism data. Bulletin of the Seismological Society of America, 100,1816–1822.

Herren, E., 1987. Zanskar shear zone: Northeast-southwest extension within the Higher Himalayas (Ladakh, India). Geology, 15, 409-413.

Hodges, K.V., Parrish, R.R., Housh, T.B., Lux, D.R., Burchfiel, B.C., Royden, L.H., and Chen, Z., 1992. Simultaneous Miocene extension and shortening in the Himalayan orogen. Science, 258, 1466-1469.

Imayama, T. and Arita, K., 2008. Nd isotopic data reveal the material and tectonic nature of theMain Central Thrust zone in Nepal Himalaya. Tectonophysics, 451, 265-281.

Kayal., J.R., Baruah, Santanu, Baruah, S., Gautam, J.L., Arefiev, S.S. and Tatevossian, R., 2011. The September 2011 Sikkim deeper centroid Mw 6.9 earthquake: Role of transverse faults in eastern Himalaya. Deep Continental Studies in India, 21,13-16.

Kellett, D.A., and D. Grujic, 2012. New insight into the South Tibetan detachment system: Not a single progressive deformation. Tectonics, 31, (doi: 10.1029/2011TC002957).

Kellett, D.A., Grujic, D., Coutand, I., Cottle, J., and Mukul, M., 2013. The South Tibetan detachment system facilitates ultra rapid cooling of granulite- facies rocks in Sikkim Himalaya. Tectonics, 32, (doi:10.1002/tect.20014).

Kohn, M.J. 2008. P-T-t data from central Nepal support critical taper and repudiate large-scale channel flow of the Greater Himalayan Sequence. Geological Society of America Bulletin, 120, 259-273.

Kohn, M.J., Paul, S.K., and Corrie, S.L., 2010. The lower Lesser Himalayan sequence: A Paleoproterozoic arc on the northern margin of the Indian plate. Geological Society of America Bulletin, 122, 323-335.

Kumar, M.R., Hazarika, P., Prasad, G.S., Singh, A., and Saha, S., 2012. Tectonic implications of the September 2011 Sikkim earthquake. Current Science, 102, 788-792.

Kündig, R., 1988. Kristallisation und Deformation i Higher Himalaya, Zanskar (NWIndien), (unpublished Ph.D. thesis), ETH Zürich, 188 p.

Kundu, A., Matin, A., and Mukul, M., 2012. Depositional environment and provenance of Middle Siwalik sediments in Tista valley, Darjiling District, Eastern Himalaya, India. Journal of Earth System Science. 121, 73-89.

Kundu, A., Matin, A., Mukul, M., Eriksson, P.G., 2011. Sedimentary facies and soft-sediment deformation structures in the Late Miocene-Pliocene Middle Siwalik Subgroup, Eastern Himalaya, Darjiling District, India. Journal of the Geological Society of India, 78, 321-336.

Larson, K.P., Gervais, F., and Kellett, D.A., 2013. A P-T-t-D discontinuity in east-central Nepal: Implications for the evolution of the Himalayan mid-crust. Lithos, 179, 275-292.

Lavé, J. and Avouac, J. P., 2001. Fluvial incision and tectonic uplift across the Himalayas of central Nepal. Journal of Geophysical Research B: Solid Earth, 106, 26561-26591.

Law, R.D., Schmid, S., and Wheeler, J., 1990. Simple shear deformation and quartz crystallographic fabrics - a possible natural example from the Torridon area of NW Scotland. Journal of Structural Geology, 12, 29–45.

Le Fort, P., 1975. Himalayas: The collided range. Present knowledge of the continental arc. American Journal of Science. 275, 1-44.

Lister, G.S., and Dornsiepen, U., 1982. Fabric transitions in the Saxony granulite terrain. Journal of Structural Geology, 4, 81–92.

Lombardo, B., and Rolfo, F., 2000. Two contrasting eclogite types in the Himalayas: implications for the Himalayan orogeny. Journal of Geodynamics, 30, 37–60, (doi:10.1016/S0264-3707(99)00026-5).

Long, S., McQuarrie, N., Tobgay, T., Rose, C., Gehrels, G. and Grujic, D., 2011a. Tectonostratigraphy of the Lesser Himalaya of Bhutan: Implications for the along-strike stratigraphic continuity of the northern Indian margin. Geological Society of America Bulletin, 123, 1406-1426.

Long, S., McQuarrie, N., Tobgay, T., Grujic, D. and Hollister, L. 2011b. Geologic Map of Bhutan, Journal of Maps, 7, 184-192. 10.4113/jom.2011.1159.

Macedo, J. and Marshak, S., 1999. The geometry of fold-thrust belt salients. Geological Society of America Bulletin, 111, 1808-1822.

Mahajan, A.K., Gupta, V., Thakur, V.C., 2012. Macroseismic field observations of 18 September 2011 Sikkim earthquake. Natural Hazards, http://dx.doi.org/10.1007/s11069-012-0170-0.

Marshak, S., 2004. Arcs, Oroclines, Salients, and Syntaxes - The origin of map-view curvature in fold-thrust belts. American Association of Petroleum Geologists Memoir, 82, 131-156.

Martin, A.J., Burgy, K.D., Kaufman, A.J., and Gehrels, G.E., 2011. Stratigraphic and tectonic implications of field and isotopic constraints on depositional ages of Proterozoic Lesser Himalayan rocks in central Nepal. Precambrian Research, 185, 1-17.

Martin, A.J., DeCelles, P.G., Gehrels, G.E., Patchett, P.J., and Isachsen, C., 2005. Isotopic and structural constraints on the location of the Main Central thrust in the Annapurna Range, central Nepal Himalaya. Geological Society of America Bulletin, 117, 926-944.

Matin, A., and Mazumdar, S., 2009. Deformation mechanisms in the frontal Lesser Himalayan Duplex in Sikkim Himalaya, India. Journal of Earth System Science, 118, 379-390.

McQuarrie, N., Robinson, D., Long, S., Tobgay, T., Grujic, D., Gehrels, G., Ducea, M., 2008. Preliminary stratigraphic and structural architecture of Bhutan: Implications for the along strike architecture of the Himalayan system. Earth and Planetary Science Letters, 272, 105-117.

McQuarrie, N., Long, S.P., Tobgay, T., Nesbit, J.N., Gehrels, G., and Ducea, M.N., 2013. Documenting basin scale, geometry and provenance through detrital geochemical data: Lessons from the Neoproterozoic to Ordovician Lesser, Greater, and Tethyan Himalayan strata of Bhutan. Gondwana Research, 23, 1491-1510.

Mishra, O.P., Chakrabortty, G.K., Singh, O.P., Ghosh, D.C., Mukherjee, K.K., and Das, P. C., 2010. A Report on Seismogenesis in the Sikkim-Darjiling Himalayas and Assimilation of Dynamic Snap Shots of the Region: Future Vulnerability: GSI Report (FSP: SEI/CHQ/CGD/2007/070), 57 p.

Mitra, G., Bhattacharyya, K. and Mukul, M., 2010. The Lesser Himalayan Duplex in Sikkim: Implications for variations in Himalayan shortening. Journal of Geological Society of India, 75, 276-288.

Mohan, A., Windley, B.F. and Searle, M.P., 1989. Geothermobarometry and development of inverted metamorphism in the Darjeeling-S ikkim region of the eastern Himalayan. Journal of Metamorphic Geology, 7, 95-110.

Montomoli, C., Iaccarino, S., Carosi, R., Langone, A., and Visonà, D., 2013. Tectonometamorphic discontinuities within the Greater Himalayan Sequence in Western Nepal (Central Himalaya): Insights on the exhumation of crystalline rocks. Tectonophysics, 608, 1349-1370.

Mottram, C.M. 2014. Crustal extrusion along the Main Central Thrust in the Sikkim Himalaya. Unpublished PhD thesis, The Open University.

Mottram, C.M., Argles, T., Parrish, R., Harris, N., Horstwood, M., and Gupta, S. 2014. Tectonic interleaving along the Main Central Thrust, Sikkim Himalaya. Journal of the Geological Society, in press.

Mukul, M., 2010. First-order kinematics of wedge-scale active Himalayan deformation: Insights from Darjiling–S ikkim– Tibet (DaSiT) wedge. Journal of Asian Earth Sciences, 39, 645-657.

Mukul, M., 2000. The geometry and kinematics of the Main Boundary thrust and related. neotectonics in the Darjiling Himalayan fold-and-thrust belt, West Bengal. Journal of Structural Geology, 22, 1261-1283.

Mukul, M., Jaiswal., M., and Singhvi, A.K., 2007. Timing of recent out-of-sequence active deformation in the frontal Himalayan wedge: Insights from the Darjiling sub-Himalaya, India. Geology, 35, 999-1003.

Nakata, T., 1989. Active faults of the Himalaya of India and Nepal. Geological Society of America Special Paper, 232, 243–264.

Nelson, K.D., Zhao, W., Brown, L.D., Kuo, J., Che, J., Liu, X., Klemperer, S.L., Makovsky, Y., Meissner, R., Mechie, J., Kind, R., Wenzel, F., Ni, J., Nabelek, J., Chen, L., Tan, H., Wei, W., Jones, A.G., Booker, J., Unsworth, M., Kidd, W.S.F., Hauck, M., Alsdorf, D., Ross, A., Cogan, M., Wu, C., Sandvol, E.A. and Edwards, M., 1996. Partially molten middle crust beneath southern Tibet: synthesis of project INDEPTH results. Science, 274, 1684–1688.

Newman, J., and Mitra, G., 1994. Fluid-influenced deformation and recrystallization of dolomite at low temperatures along a natural fault zone, Mountain City window, Tennessee. Geological

Society of American Bulletin, 106, 1267-1280.
Ni, J. and Barazangi, M., 1984. Seismotectonics of the Himalayan Collision Zone: Geometry of the underthrusting Indian plate beneath the Himalaya. Journal of Geophysical Research, 89, 1147-1163.
Pan, G., Ding, J., Yao, D., and Wang, L., 2004. Geological map of Qinghai-Xiang (Tibet) plateau and adjacent areas (1:1,500,000), Chengdu Institute of Geology and Mineral Resources, China Geological Survey, Chengdu Cartographic Publishing House, Chengdu, China.
Pandey, M.R., Tandulkar, R.P., Avouac, J.P., Vergne, J. and Heritier. T., 1999. Seismotectonics of the Nepal Himala ya from a local seismic network. Journal of Asian Earth Sciences, 17, 703-712.
Parrish, R.R., and Hodges, K.V., 1996. Isotopic constraints on the age and provenance of the Lesser and Greater Himalayan sequences, Nepalese Himalaya. Geological Society of America Bulletin, 108, 904-911.
Paul, D.K., Chandy, K.C., Bhalla, J.K., Prasad, R., and Sengupta, P. 1982. Geochronology and geochemistry of the Lingtse Gneiss, Darjiling-Sikkim Himalaya. Indian Journal of Earth Sciences, 9, 11-17.
Paul, D.K., McNaughton, N.J., Chattopadhyay, S., and Ray, K.K., 1996. Geochronology and geochemistry of the Lingtse gneiss, Darjiling-S ikkim Himalaya: Revisited. Journal of the Geological Society of India, 48, 497-506.
Pêcher, A., 1989. The metamorphism in the central Himalaya. Journal of Metamorphic Geology, 7, 31-41.
Powers, P.M., Lillie, R.J. and Yeats, R.S., 1998. Structure and shortening of the Kangra and Dehra Dun re-entrants, Sub-Himalaya, India. Geological Society of America Bulletin, 110, 1010-1027.
Pradhan, R., Prajapati, S. K., Chopra, S., and Kumar, A., 2013. Causative source of Mw; 6.9 Sikkim-Nepal border earthquake of September 2011: GPS baseline observations and strain analysis. Journal of Asian Earth Sciences, 70-71, 179–192.
Rajendran, K., Rajendran, C.P., Thulasiraman, N., Andrews, Ronia and Sherpa, N., 2011. The 18 September 2011, North Sikkim earthquake. Current Science, 101, 1475–1479. Raju, P.S., Rao, N.P., Singh, A., and Kumar, M.R., 2007. The 14 February 2006 Sikkim earthquake of magnitude 5.3. Current Science, 93, 848–850.
Richards, A., Argles, T., Harris, N., Parrish, R., Ahmad, T., Darbyshire, F. and Draganits, E. 2005. Himalayan architecture constrained by isotopic tracers from clastic sediments. Earth and Planetary Science Letters, 236, 773-796.
Richards, A., Parrish, R., Harris, N., Argles, T. and Zhang, L. 2006. Correlation of lithotectonic units across the eastern Himalaya, Bhutan. Geology, 34, 341-344.
Ring, U., Glodny, J., Will, T., and Thomson, S., 2007. An Oligocene extrusion wedge of blueschist- facies nappes on Evia, Aegean Sea, Greece: implications for the early exhumation of high-pressure rocks. Journal of the Geological Society, 164, 637-652.
Robinson, D.M., DeCelles, P.G., Patchett, P.J., and Garzione, C.N., 2001. The kinematic evolution of the Nepalese Himalaya interpreted from Nd isotopes. Earth and Planetary Science Letters, 192, 507-521.
Rolfo, F., Carosi, R., Montomoli, C., and Visonà, D., 2008. Discovery of granulitized eclogite in North Sikkim expands the Eastern Himalaya high-pressure province. Himalayan Journal of Sciences, 5, 126–127, (doi:10.3126/hjs.v5i7.1312).
Rubatto, D., S. Chakraborty, and Dasgupta, S., 2013. Timescales of crustal melting in the Higher Himalayan Crystallines (Sikkim, Eastern Himalaya) inferred from trace element-constrained monazite and zircon chronology. Contributions to Mineralogy and Petrology, 165, 349-372.
Sahoo, P.K., Kumar, S. and Singh, R.P., 2000. Neotectonic study of Ganga and Yamuna tear faults, NW Himalaya, using remote sensing and GIS. International Journal of Remote Sensing, 21, 499-518.
Schelling, D., and Arita, K., 1991. Thrust tectonics, crustal shortening and the structure of the far-eastern Nepal Himalaya. Tectonics, (doi:10.1029/91TC01011).
Schmid, S.M., and Casey, M., 1986. Complete fabric analysis of some commonly obserbed quartz c-axis patterns, in Mineral and Rock Deformation, Laboratory studies, Hobbs, B.E. and Heard, H.C., eds. Geophysical Monograph Series, 36, 263-286.
Searle, D., Simpson, R.L., Law, R.D., Parrish, R.R., and Waters, D.J., 2003. The structural geometry, metamorphic and magmatic evolution of the Everest massif, High Himalaya of Nepal-South Tibet. Journal of the Geological So-

ciety, London, 160, 345-366.

Searle, M.P., Law, R.D., Godin, L., Larson, K.P., Streule, M.J., Cottle, J.M. and Jessup, M.J., 2008. Defining the Himalayan Main Central Thrust in Nepal. Journal of the Geological Society, 165, 523-534.

Srivastava, P. and Mitra, G., 1994. Thrust geometries and deep structure of the outer and lesser Himalaya, Kumaon and Garhwal (India): Implications for evolution of the Himalayan fold-and-thrust belt. Tectonics, 13, 89-109.

Tobgay, T., Long, S., McQuarrie, N., Ducea, M.N. and Gehrels, G., 2010. Using isotopic and chronologic data to fingerprint strata: Challenges and benefits of variable sources to tectonic interpretations, the Paro Formation, Bhutan Himalaya. Tectonics, 29, (doi:10.1029/2009TC002637).

Warren, C.J., Grujic, D., Kellett, D.A., Cottle, C., and Jamieson, R.A., 2011. Probing the depths of the India-Asia collision: U-Th-Pb monazite chronology of granulites from NW Bhutan. Tectonics, 30, (doi:10.1029/2010TC002738).

Webb, A.A.G., Yin, A., and Dubey, C.S., 2013. U-Pb zircon geochronology of major lithologic units in the eastern Himalaya: Implications for the origin and assembly of Himalayan rocks. Geological Society of America Bulletin, 125, 499-522.

Wernicke, B., and Burchfiel, B.C., 1982. Modes of extensional tectonics. Journal of Structural Geology, 4, 105-115.

Wu, C., Nelson, K.D., Wortman, G., Samson, S.D., Yue, Y., Li, J., Kidd, W.S.F., and Edwards, M.A., 1998. Yadong cross structure and South Tibetan Detachment in the east central Himalaya (89º90ºE). Tectonics, 17, 28-45.

Xypolias, P., and Kokkalas, S., 2006. Heterogeneous ductile deformation along a midcrustalextruding shear zone: an example from the External Hellenides (Greece): in Channel Flow, Ductile Extrusion and Exhumation in Continental Collision Zones, Law, R., Searle, M.P., Godin, L., ed. Special Publications: London, Geological Society, 268, 497-516.

Yin A., 2006. Cenozoic tectonic evolution of the Himalayan orogen as constrained by along-strike variation of structural geometry, exhumation history, and foreland sedimentation. Earth Science Reviews, 76, 1–131.